Grey Horse Channel

Azamethiphos Dispersion Modelling Report

[redacted]

[redacted]

CAR/L/1025571/V8

August 2021

› Mowi Scotland

OFFICE
Mowi, [redacted]

POSTAL
Mowi, [redacted]

PHONE [redacted]

FAX

MAIL [redacted]

WEB [redacted]

CONTENTS

List of Figures

List of Tables

EXECUTIVE SUMMARY

Dispersion model simulations have been performed to assess whether bath treatments at Grey Horse Channel salmon farm will comply with pertinent environmental quality standards. A realistic treatment regime, with 1 pen treatment a day, was simulated. For 100 metre circumference pens each pen required 477 g of azamethiphos (the active ingredient in Salmosan, Salmosan Vet and Azasure) for treatment, resulting in a daily release of 477 g and a total discharge over 14 days of 6.678 kg. Simulations were performed separately for modelled neap and spring tides and a combined neap simulation, and the sensitivity of the results to key model parameters was tested.

The model results confirmed that the treatment scenario proposed, with a daily release of no more than 477 g, should comply with the EQS. The peak concentration during the baseline simulation after 384 hours (72 hours after the final treatment) was less than 0.1 µg/L, the maximum allowable concentration, and the area where concentrations exceeded the EQS of 0.04 µg/L was substantially less than the allowable 0.5 km^2. The baseline simulation presented here was designed to be very conservative. Results are summarised in Table 1.

The 24-hour mass is substantially larger than the amount predicted by the standard bath model, but the latter is known to be highly conservative, because it does not account for horizontal shearing and dispersion of medicine patches due to spatially-varying current fields, processes which are known to significantly influence dispersion over time scales greater than a few hours.

Table 1. Summary of Results

SITE DETAILS			
Site Name:		Grey Horse Channel	
Site location:		Sound of Harris	
Peak biomass (T):		1,750	
CAGE DETAILS			
Number of pens:		14	
Cage dimensions:		100m Circumference	
Working Depth (m):		12	
Cage group configuration:		2 x 7, 60m matrix	
HYDROGRAPHIC SUMMARY		**ID210**	**ID342**
Surface Currents	**Grey Horse Channel**	**Mar-Jul 2018**	**Jun-Aug 2020**
	Mean Speed (m/s)	0.108	0.182
	Residual Speed (m/s)	0.005	0.037
	Residual Direction (°G)	008	108
	Tidal Amplitude Parallel (m/s)	0.175	0.278
	Tidal Amplitude Normal (m/s)	0.045	0.091
	Major Axis (°G)	310	130
BATH TREATMENTS			
Recommended consent mass - 3hr Azamethiphos (g)		477	
Recommended consent mass - 24hr Azamethiphos (g)		477	

1 INTRODUCTION

This report has been prepared by Mowi Scotland Ltd. to meet the requirements of the Scottish Environment Protection Agency (SEPA) for an application to use Azamethiphos bath treatments on a marine salmon farm near Cheesebay, North Uist (Figure **1**). The report presents results from coupled hydrodynamic and particle tracking modelling to describe the dispersion of bath treatments to determine EQS-compliant quantities for the current site biomass and equipment. The modelling procedure follows as far as possible guidance presented by SEPA in June 2019 (SEPA, 2019).

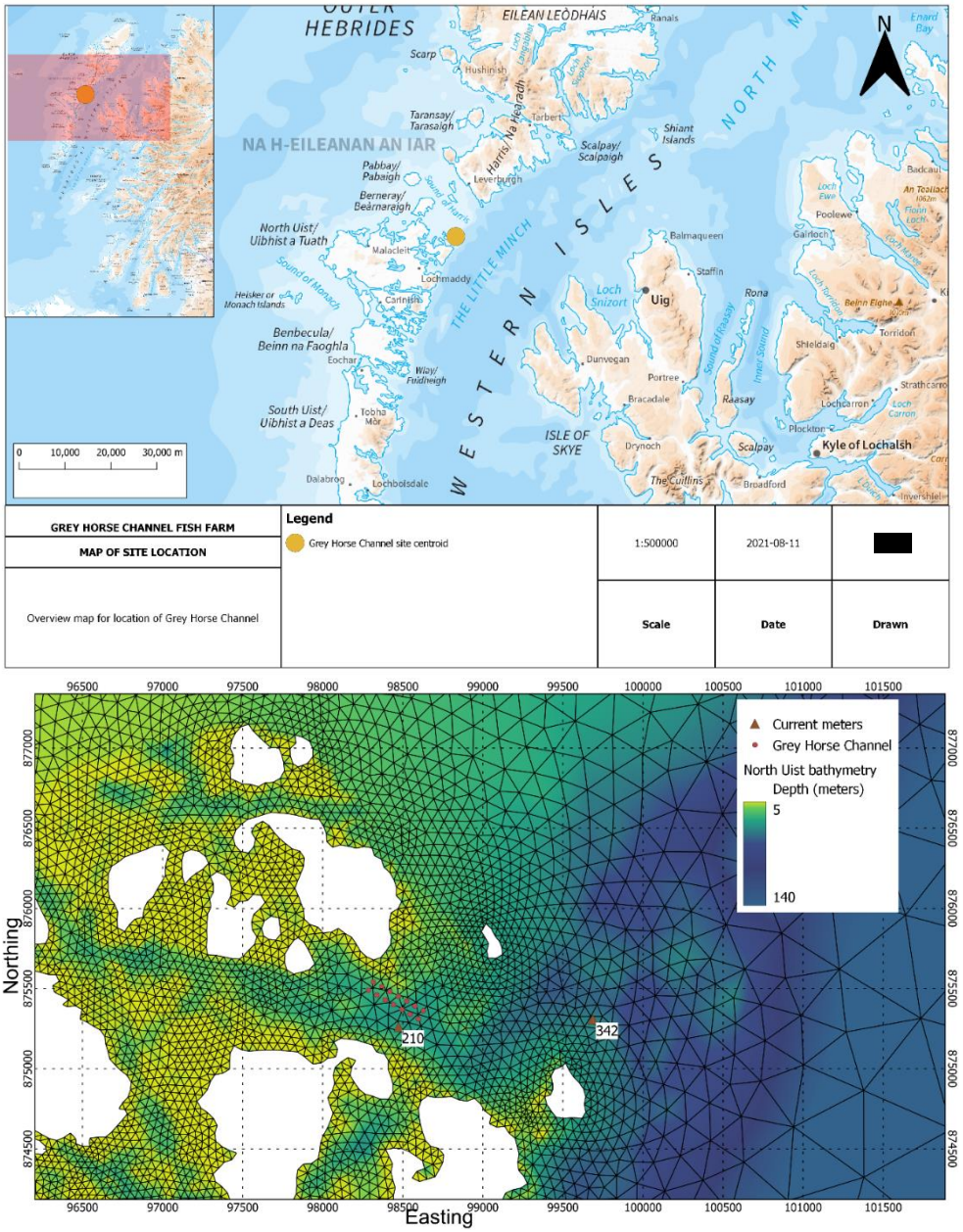

Figure 1. Location of Grey Horse Channel salmon farm (top) and the location of the ADCP deployments in 2018 and 2020 (▲) relative to the current pen positions (**o**).

1.1 Site Details

The site is situated in Grey Horse Channel North East of Cheese Bay, North Uist (Figure 1). Details of the site are provided in Table 2 (Grey Horse Channel). The receiving water is defined as the Sound of Harris.

Table 2. Project Information – Grey Horse Channel

SITE DETAILS	
Site Name:	Grey Horse Channel
Site location:	Sound of Harris
Peak biomass (T):	1,750
Proposed feed load (T/yr):	4471.25
Proposed treatment use:	Azamethiphos
CAGE DETAILS	
Group location:	NF98457542
Number of cages:	14
Cage dimensions:	100m circumference
Grid matrix (m)	65
Working Depth (m):	12
Cage group configuration:	2x7
Cage group orientation (°G):	120.6
Cage group distance to shore (km):	0.19
Water depth at site (m):	19 – 22 m
HYDROGRAPHIC DATA	
	ID210
Current meter position:	98474E, 875261N
Depth at deployment position (m):	18.53
Duration of record (days):	119
Start of record:	13-Mar-2018
End of record:	07-Oct-2018
Current meter averaging interval (min):	20
Magnetic correction to grid North:	-4.19

2 METHODS

2.1 Model Selection

The modelling approach adopted a coupled hydrodynamic and particle tracking method, whereby water currents in the region, modelled using a calibrated hydrodynamic model, advected particles representing the topical medicine around the model domain. Turbulent eddy diffusion was modelled using a random walk method. Outputs from the modelling were derived to assess the dispersion of the medicine following treatments against statutory Environmental Quality Standards. The modelling approach is described in full in Annex A and is only summarised here.

For the hydrodynamics, the RiCOM model was used. RiCOM (River and Coastal Ocean Model) is a general-purpose hydrodynamics and transport model, which solves the standard Reynolds-averaged Navier-Stokes equation (RANS) and the incompressibility condition, applying the hydrostatic and Boussinesq approximations (Walters and Casulli, 1998). It has been tested on a variety of benchmarks against both analytical and experimental data sets. The model has been previously used to investigate the inundation risk from tsunamis and storm surge on the New Zealand coastline, the effects of mussel farms on current flows, and, more recently in Scotland to study tidal energy resource and the effects of energy extraction on the ambient environment (McIlvenny et al., 2016; Gillibrand et al., 2016).

The mathematical equations are discretized on an unstructured grid of triangular elements which permits greater resolution of complex coastlines, such as typically found in Scotland. Therefore, greater spatial resolution in near-shore areas can be achieved without excessive computational demand. Full details of the RiCOM model and simulations are given in Annex A.

For the particle tracking component, Mowi's in-house model unptrack (Gillibrand, 2020) was used. The model used the hydrodynamic flow fields from the RiCOM model simulations. This model has been used previously to simulate sea lice dispersal (Gillibrand and Willis, 2007), the development of a harmful algal bloom (Gillibrand et al., 2016) and the dispersion of cypermethrin from a fish farm (Willis et al., 2005). The approach for veterinary medicines is the same as for living organisms, except that medicine has no biological behaviour but instead undergoes chemical decay: the numerical particles in the model represent "droplets" of medicine of known mass, which reduces over time at a rate determined by a specified half-life. Particles are released at cage locations at specified times, according to a treatment schedule. The number of particles combined with their initial mass represents the mass of medicine required to treat a cage. The particles are then subject to advection, from the modelled flow fields, and horizontal and vertical diffusion. The choice of horizontal diffusion coefficient was informed by dye release experiments in the Grey Horse Channel area. A dye release was performed at Grey Horse Channel. After 72 hours, concentrations of medicine are calculated and compared with the relevant Environmental Quality Standard (EQS). Here, we have modelled the dispersion of azamethiphos following a treatment scenario to illustrate the quantities of medicine that disperse safely in the environment.

2.2 Model Domain and Boundary Conditions

The unstructured mesh used in the model was adapted from the East Coast of Lewis and Harris (ECLH) sub-model mesh of the Scottish Shelf Model (SSM; MS, 2016). Model resolution was enhanced in the Sound of Harris region particularly around the Mowi Scotland sites near Cheese Bay. The domain and mesh are shown in Figure 2, with the area around Cheese Bay shown in Figure 3.

The mesh was not refined down to 25m specifically in the area of the cages, since dispersion is not a localised process, unlike particulate deposition, and takes place over a much wider area. However, the mesh, like the original ECLH mesh, is relatively highly resolved in the Little Minch area (Figure 3) and is completely adequate for modelling dispersion of solutes. The spatial resolution of the model varied from 25m in some inshore waters to 5 km along the open boundary. In total, the model consisted of 35,986 nodes and 66,301 triangular elements.

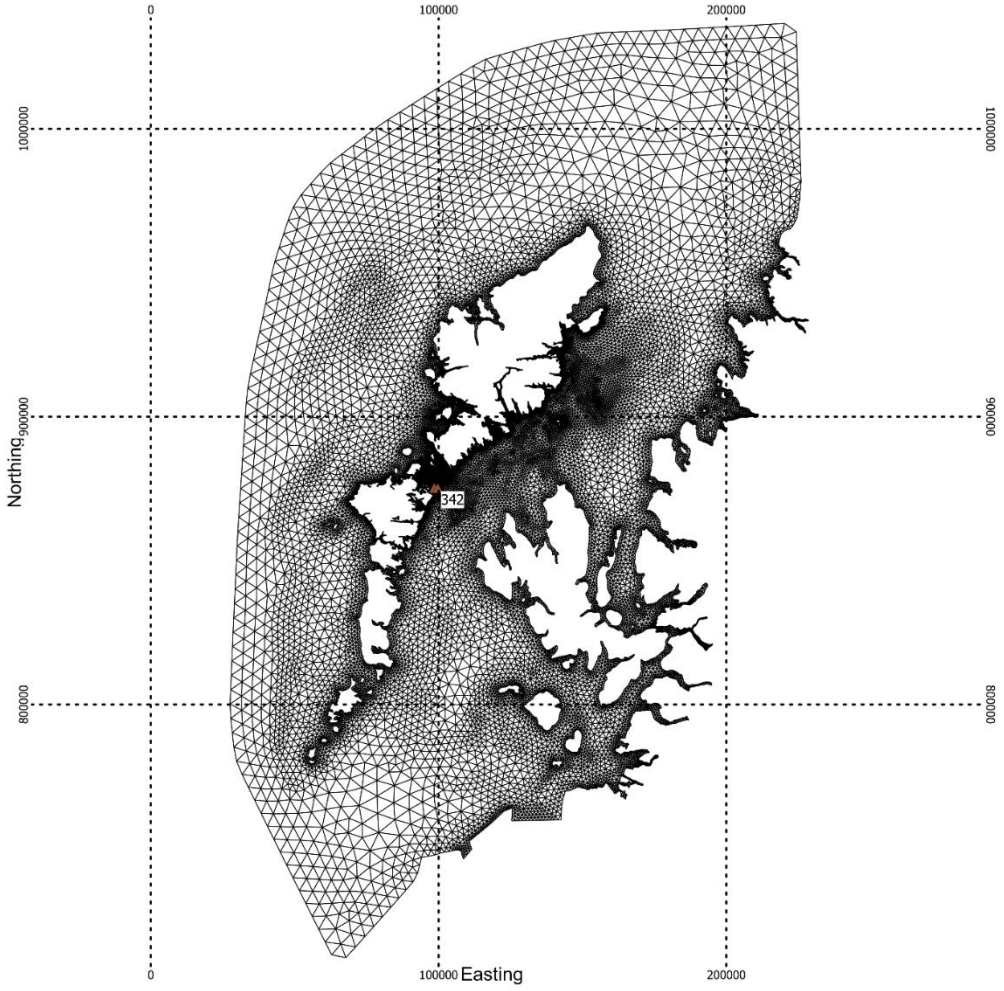

Figure 2. The modified ECLH domain and mesh used in the North Uist modelling.

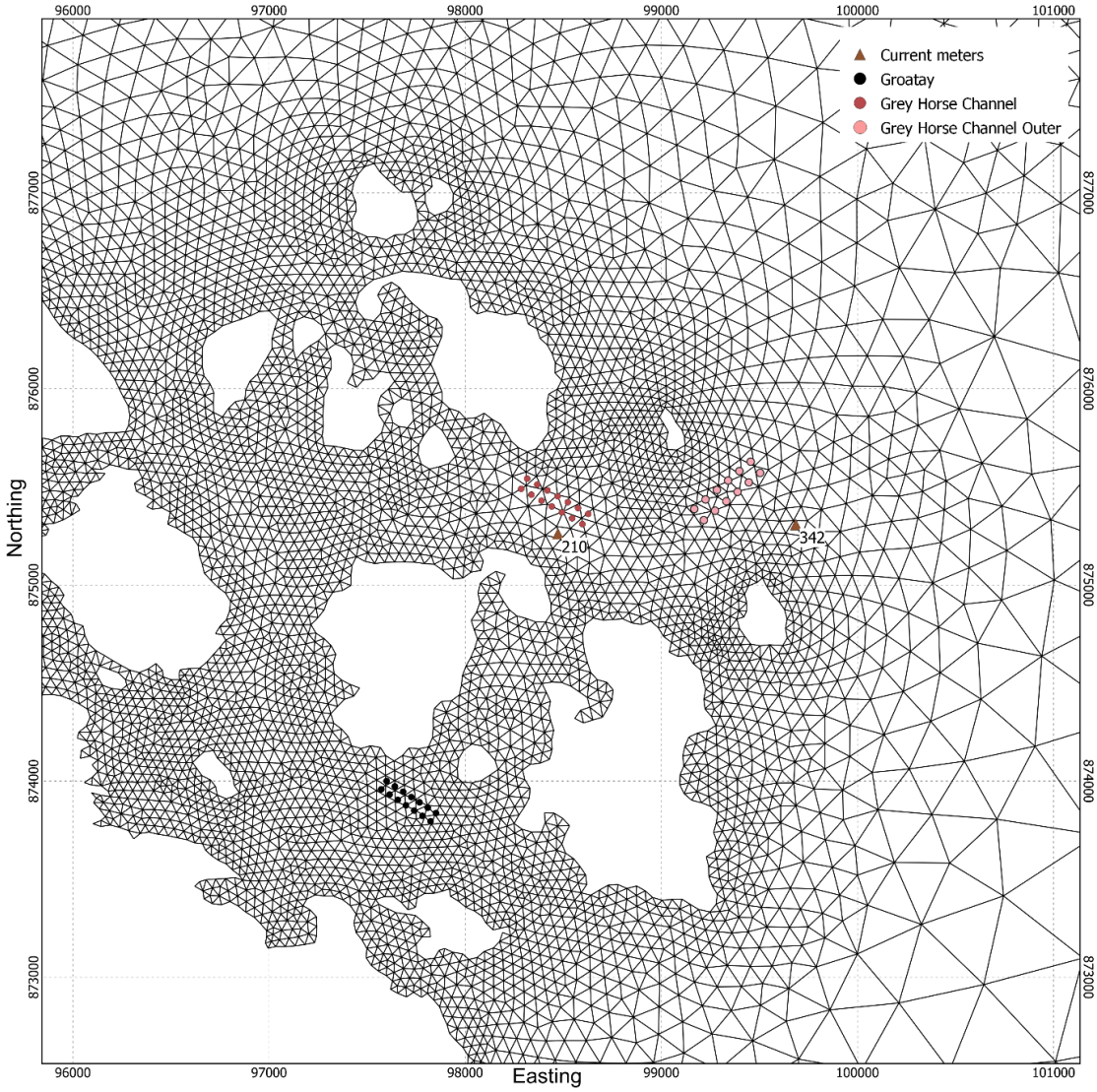

Figure 3. The model mesh in the area around the Cheese Bay sites. The pen locations and current meter positions are indicated.

Bathymetry was taken from the original ECLH model and interpolated onto the new nodal locations and supplemented in the Sound of Harris using multibeam data available from the Admiralty's Seabed Mapping Service (https://seabed.admiralty.co.uk/). Given that topical medicine dispersion occurs in the upper water column, it was not deemed necessary to use very detailed bathymetry data in the immediate vicinity to the cages.

The model was forced along its open boundary by twelve tidal constituents (O_1, K_1, K_2, Q_1, P_1, M_2, M_4, MM, MSF, MF, S_2, N_2, K_2), amplitudes and phase of which were obtained from the full SSM. Spatially- and temporally-varying wind speed and direction data were taken from the ERA5 global reanalysis dataset for the required simulation periods (https://www.ecmwf.int/en/forecasts/datasets/reanalysis-datasets/era5).

Stratification is relatively weak in this location, given the strong tidal flows in the area, and the model was run in 2D vertically-averaged mode.

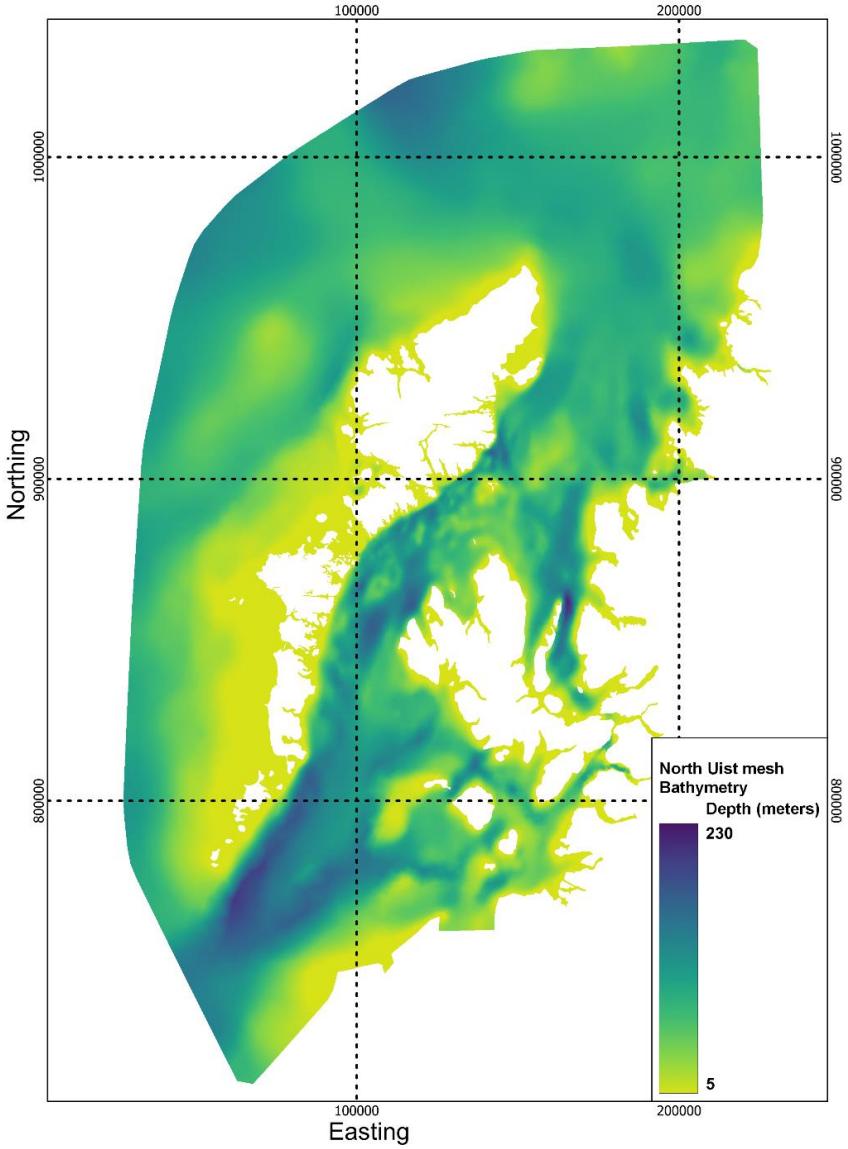

Figure 4. Bathymetry (meters), in the ECLH North Uist domain.

2.3 Hydrodynamic Model Calibration

The hydrodynamic model was calibrated against current data and seabed pressure data, measured at Grey Horse Channel and Grey Horse Channel Outer sites using Acoustic Doppler Current Profilers (ADCP). Data are available at two locations (Figure 1) from:

(i) 13th March – 10th July 2018 (ID210)
(ii) 9th June – 26thnd August 2020 (ID342)

In total, the data extends over 198 days. Calibration was performed in a standard fashion, with bed friction adjusted to obtain the best fit against the sea surface height and current data. The model ran for the same period as the observations and the modelled surface elevation and velocity at the three data locations were evaluated against the observed data. Details of the calibrations are given in Annex A.

The unptrack model uses the same unstructured mesh as the hydrodynamic model, and reads the flow fields directly from the hydrodynamic model output files. Therefore, no spatial or temporal interpolation of the current fields is required, although current velocities are interpolated to particle locations within unptrack.

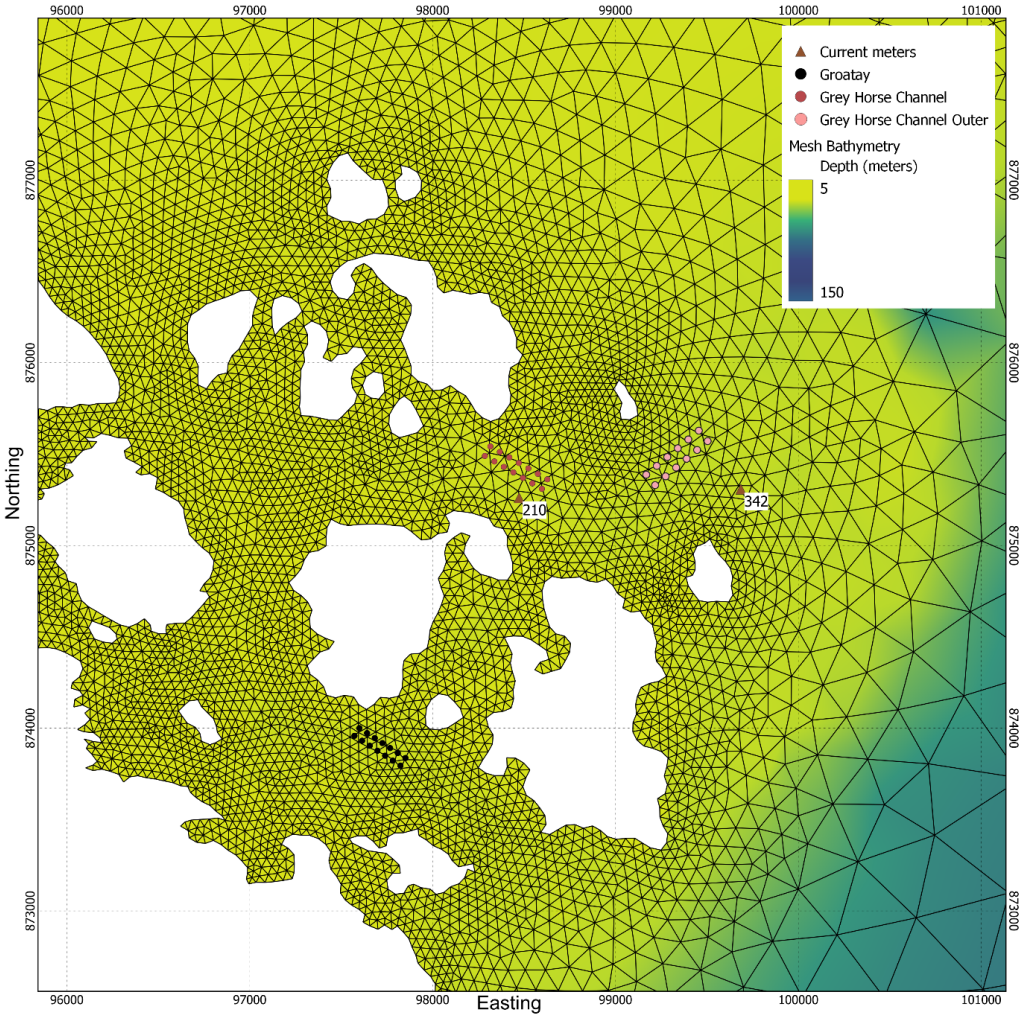

Figure 5. Localised bathymetry around Grey Horse Channel area in the modified ECLH domain. The pen locations of Grey Horse Channel, Grey Horse Channel Outer and Groatay sites are marked.

2.4 Medicine Dispersion Modelling

The medicine dispersion modelling, performed using the unptrack model (Gillibrand, 2020), simulates the dispersion of patches of medicine discharged from cages following treatment using tarpaulins. The treatment scenario assumed 4 cages can be treated per day at 3-hour intervals. This gives adequate time for installation of tarpaulins, dosage, and removal of tarpaulins for each cage.

To simulate the worst-case scenario, the dispersion modelling was initially conducted using flow fields over a period of eight days centred on a small neap tidal range taken from the hydrodynamic model simulations. This is assumed to be the least dispersive set of ambient conditions, when medicine dispersion is least likely to meet the required EQS. Later simulations tested dispersion during spring tides.

A treatment depth of 5 m was chosen as a realistic net depth during application of the medicine for a 100m pen. The initial mass released per pen was calculated from the reduced cage volume and a treatment concentration of 120 µg/L, with a total mass of 6.685 kg of azamethiphos released during treatment of each farm. Particles were released from random positions within a cage radius of the centre and within the 0 – 5 m depth range. The simulations used *ca.* 1,114,078 numerical particles in total, each particle representing 6 mg of azamethiphos.

Each simulation ran for a total of 408 hours. This covered the treatment periods (147 hours), a dispersion period to the EQS assessment after 384 hours for GHC (72 hours after the final treatment), and an extra 24 hours to check for chance concentration peaks. At every hour of the simulation, particle locations and properties (including the decaying mass) were stored and subsequently concentrations calculated.

From the calculated concentration fields, time series of two metrics were constructed for the whole simulation:

(i) The maximum concentration (µg/L) anywhere in the mesh;
(ii) The area (km^2) where the EQS was exceeded;

These results were used to assess whether the EQS or MAC was breached after the allotted period (72 hours after the final treatment).

Sensitivity analyses were conducted to assess the effects of:

(i) Medicine half-life
(ii) Horizontal diffusion coefficient, K_H
(iii) Vertical diffusion coefficient, K_V
(iv) Time of release

The dispersion simulations were performed separately over neap and spring tides during 2018 (ID210 - Figure 6) and 2020 (ID342).

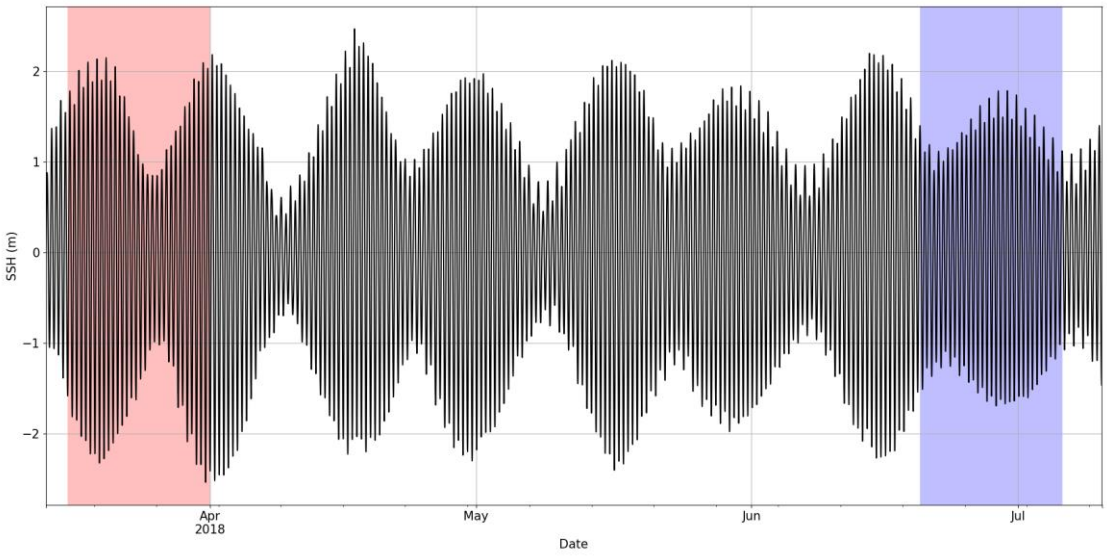

Figure 6. Sea surface height (SSH) at Grey Horse Channel from 13th Mar – 10th Jul 2018 (ID210). Dispersion simulations were performed over periods of spring tides (highlighted in red) and neap tides (blue).

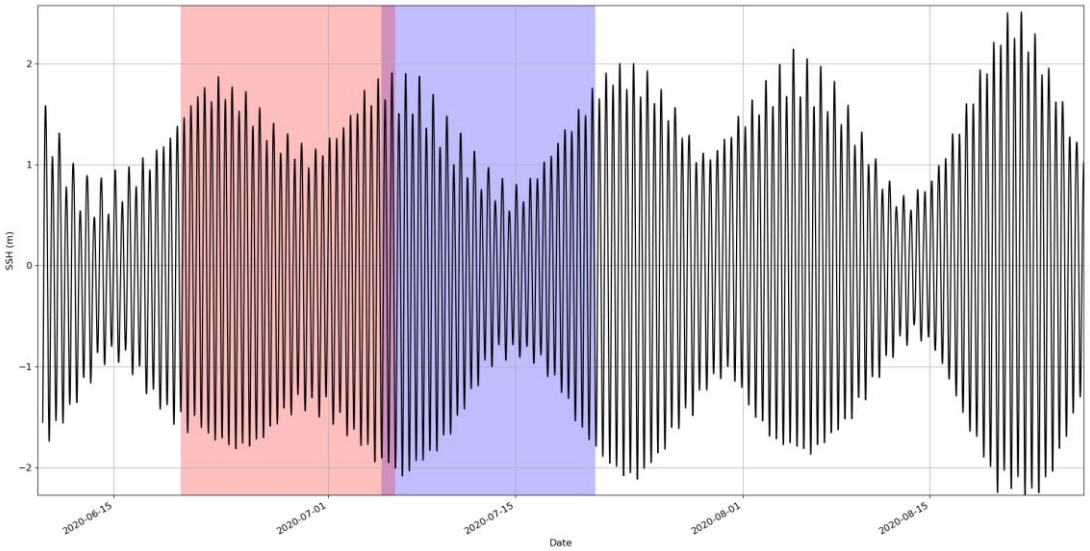

Figure 7. Sea surface height (SSH) at Grey Horse Channel Outer from 9th June – 26th Aug 2020 (ID342). Dispersion simulations were performed over periods of spring tides (highlighted in red) and neap tides (blue).

2.5 Medicine Dispersion Simulations

The pen locations and details of the medicine source for Grey Horse Channel are listed in Table 3. The time of release is relative to the start of the neap or spring period highlighted in Figure 6 and Figure 7

Table 3. Details of the treatment simulated by the dispersion model for Grey Horse Channel. The release time is relative to the start of the neap or spring period highlighted in Figures 6 and 7.

Pen	Easting	Northing	Net Depth (m)	Treatment Mass (g)	Release Time (hr)
1	98349	875512	5	477.46	0
2	98323	875458	5	477.46	24
3	98400	875486	5	477.46	48
4	98375	875433	5	477.46	72
5	98453	875461	5	477.46	96
6	98427	875405	5	477.46	120
7	98504	875436	5	477.46	144
8	98479	875382	5	477.46	168
9	98555	875409	5	477.46	192
10	98532	875356	5	477.46	216
11	98604	875383	5	477.46	240
12	98582	875328	5	477.46	264
13	98656	875358	5	477.46	288
14	98633	875302	5	477.46	312

The simulations performed are listed in Table 4. All simulations used the release schedule and quantities outlined in Table 3. In Runs 7 – 12, the release schedule was set back by a number of hours to investigate the effect of tidal state at the time of release on the results. Results for these simulations are still presented in terms of time relative to the first release.

Table 4. Dispersion model simulation details for the treatment simulations of 14 pens at Grey Horse Channel.

Set	Run No.	$T_{1/2}$ (h)	K_H (m^2 s^{-1})	K_V (m^2 s^{-1})	Start Time
Neap Tides, Start Day = 27 (5th July 2020– ID342)					
Baseline	1	134.4	0.1	0.001	00:00
1	2	213.6	0.1	0.001	00:00
	3	55.2	0.1	0.001	00:00
2	4	134.4	0.05	0.001	00:00
	5	134.4	0.2	0.001	00:00
3	6	134.4	0.1	0.0025	00:00
	7	134.4	0.1	0.0050	00:00
	8	134.4	0.1	0.001	00:00 – 6 h
	9	134.4	0.1	0.001	00:00 – 4 h
4	10	134.4	0.1	0.001	00:00 – 2 h
	11	134.4	0.1	0.001	00:00 + 2 h
	12	134.4	0.1	0.001	00:00 + 4 h
	13	134.4	0.1	0.001	00:00 + 6 h
Spring Tides, Start Day = 12 (20th June 2020 – ID342)					
	14	134.4	0.1	0.001	00:00
	15	213.6	0.1	0.001	00:00
5	16	55.2	0.1	0.001	00:00
	17	134.4	0.05	0.001	00:00
	18	134.4	0.2	0.001	00:00
	19	134.4	0.1	0.0025	00:00
	20	134.4	0.1	0.0050	00:00
Neap Tides, Start Day = 100 (6th June 2018 – ID210)					
	21	134.4	0.1	0.001	00:00
	22	213.6	0.1	0.001	00:00
	23	55.2	0.1	0.001	00:00
6	24	134.4	0.05	0.001	00:00
	25	134.4	0.2	0.001	00:00
	26	134.4	0.1	0.0025	00:00
	27	134.4	0.1	0.0050	00:00

2.6 Diffusion Coefficients

Selection of the horizontal diffusion parameter, K_H, was guided by dye releases conducted in the Western Isles region by Anderson Marine Surveys Ltd. A dye release was carried out at Grey Horse Channel on 24th July 2020. Dye tracking studies proceed by releasing a known quantity of dye into the sea, and then attempting to map the resulting dye patch as it disperses over time by deploying a submersible fluorometer from a boat. Each survey of the patch takes a finite amount of time (typically less than 30 minutes) and is usually made up of several transects which attempt to criss-cross the patch. An estimate of horizontal diffusivity can be made from each transect, but the location of the transect relative to the centre of the patch (and the highest concentrations) is often uncertain. The estimates of horizontal diffusivity shown in Figure 8 come from these individual transects.

The analysis method is based on estimating the diffusion from individual transects through the dye patch from the variance in the dye concentrations along the transect. The dye survey gave an overall mean horizontal diffusivity of 0.094 m^2 s^{-1} for this location. There is considerable scatter in the data (Figure 8), arising from the difficulty of tracking dye in the marine environment which renders individual values highly uncertain.

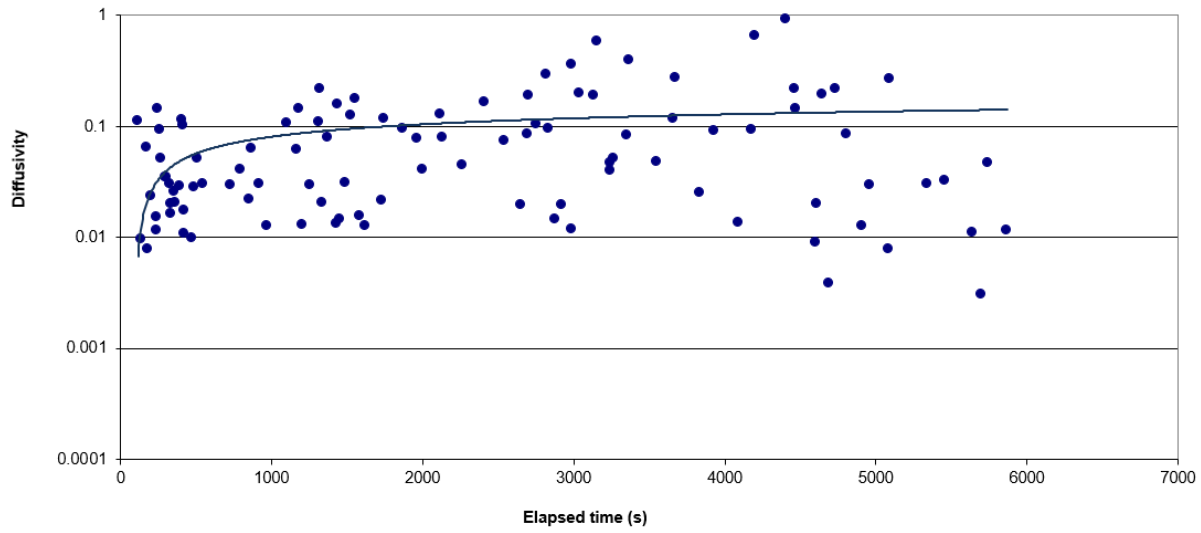

Figure 8. Estimated horizontal diffusivity (m^2 s^{-1}) from dye release experiments at Grey Horse Channel on 24th July 2020. The mean diffusivity was 0.094 m^2 s^{-1}.

A second method of analysis is also presented here. According to Fickian diffusion theory (Lewis, 1997), the maximum concentration, C_{max} in a patch of dye decreases with time according to:

$$C_{max} = \frac{M}{4\pi HKt} \quad (1)$$

where M is the mass (kg) of dye released, H is a depth of water (m) over which the dye is assumed to mix vertically, K is the horizontal diffusivity (m^2 s^{-1}), assumed equal in x- and y-directions, and t is the time elapsed since release (s). The maximum concentration measured during each post-release survey should fall according to Equation (1) and allow an estimate of K to be made.

We have identified the maximum concentration measured in each post-release survey (each comprised of a number of individual transects) and plotted the maximum concentration from each transect against the nominal time for that survey transect (typically accurate to ±1 minute). The results are shown in Figure 9. A nominal mixed depth of H = 5m was used (see also Dale et al., 2020).

The results support the notion that horizontal diffusivity in the Scottish marine environment is typically greater than 0.1 m^2 s^{-1}. The observed maximum concentrations, particularly after

about 30 minutes (1800s), fall faster than a diffusivity of 0.1 m^2 s^{-1} would imply, indicating greater diffusion. There is considerable uncertainty in the data, because it is difficult during dye surveys to repeatedly measure the point of peak concentration.

A number of dye releases have been conducted for Mowi Scotland Ltd in recent years to assess horizontal diffusivity at salmon farm sites, which collectively indicate that 0.1 m^2 s^{-1} is a reasonably conservative estimate for horizontal diffusivity in Scottish coastal waters. A similar conclusion was reached by Dale et al (2020) following dye releases conducted in Loch Linnhe and adjacent waters.

As such, the model simulations described here were conducted using a value of K_H = 0.1 m^2 s^{-1} which provided some conservatism in the results; however, the sensitivity of the model to K_H was explored, with simulations with K_H = 0.05 m^2 s^{-1} and K_H = 0.2 m^2 s^{-1} also performed and reported.

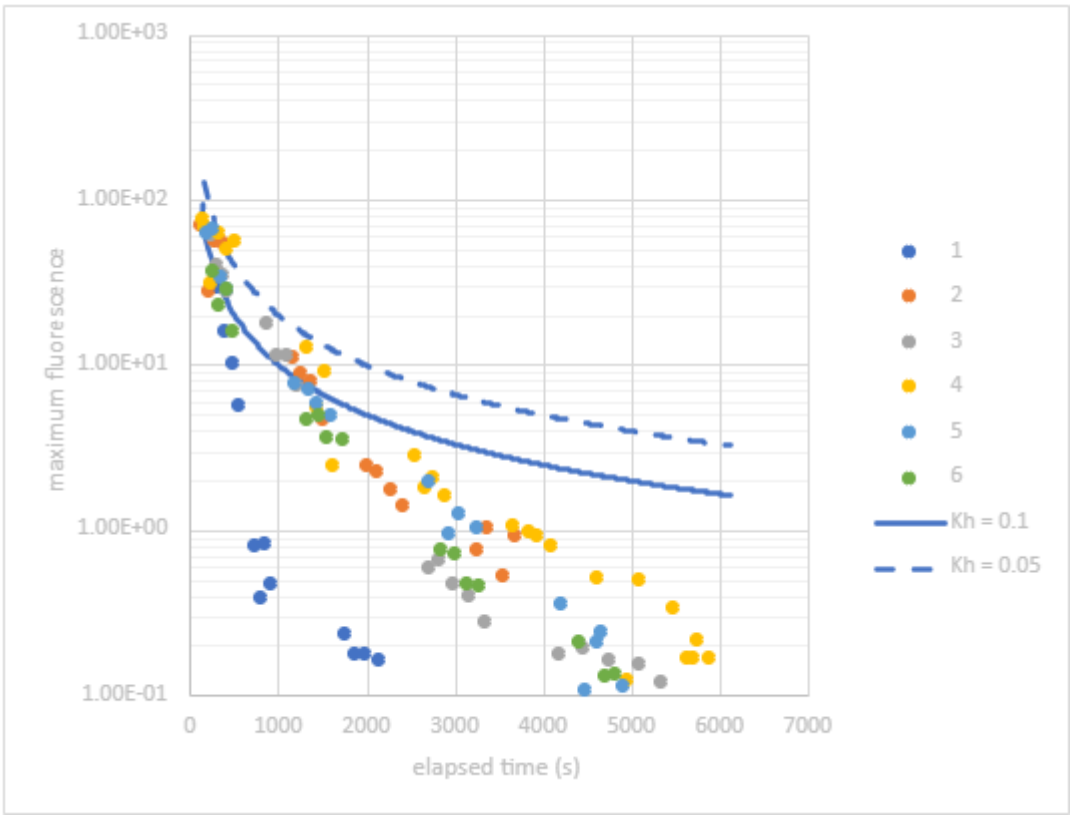

Figure 9. Maximum fluorescence measured along individual transects following six dye releases at the GHC site in July 2020. The blue lines indicate the rate at which the maximum concentration would fall at different horizontal diffusivities.

2.7 Cumulative modelling

2.7.1 Grey Horse Channel and Grey Horse Channel Outer

The site at Grey Horse Channel is managed by Mowi Scotland together with the neighbouring site at Grey Horse Channel Outer. Initial modelling simulated simultaneous treatments at both sites i.e., a total of two medicine releases per day. The releases at Grey Horse Channel (Table 5) mirrored those at Grey Horse Channel (Table 3) but starting 48 hours later to Grey Horse Channel Outer to account for the two fewer pens (12 x 120m pens). Simultaneous releases at both sites were made for the baseline neap simulation in Table 4. The results are reported in §3.7.1

Table 5. Details of the treatments at Grey Horse Channel Outer, in addition to those at Grey Horse Channel, simulated by the dispersion model. The release time is relative to the start of the neap or spring periods highlighted in Figure 6 and Figure 7.

Pen	Easting	Northing	Net Depth (m)	Treatment Mass (g)	Release Time (hr)
1	99168	875388	5	688	48
2	99217	875330	5	688	72
3	99224	875438	5	688	96
4	99274	875378	5	688	120
5	99282	875486	5	688	144
6	99330	875431	5	688	168
7	99338	875534	5	688	192
8	99387	875480	5	688	216
9	99394	875583	5	688	240
10	99444	875526	5	688	264
11	99450	875634	5	688	288
12	99500	875576	5	688	312

2.7.2 Groatay

Finally, a simulation also including medicine releases at the other active Mowi Scotland site in Cheesebay with a consent to discharge azamethiphos, Groatay, was performed. The 24-hour medicine consent for azamethiphos for Groatay, 609.1 g, is sufficient to treat one pen per day. The simulated treatments at Groatay were modelled to finish at the same time as coincident treatments at Grey Horse Channel Outer and Grey Horse Channel (Table 6), such that the EQS was applied as previously. The total mass of azamethiphos released across the three sites in these simulations was 21.6196 kg. Simulations were performed for neap tides, using baseline conditions ($T_{1/2}$ = 134.4 h, K_H = 0.1 m^2/s, K_V = 0.001 m^2/s). Results are presented in §3.7.2.

Table 6. Details of the treatments at Groatay, in addition to those at Grey Horse Channel and Grey Horse Channel Outer, simulated by the dispersion model. The release time is relative to the start of the neap or spring periods highlighted in Figure 6 and Figure 7.

Pen	Easting	Northing	Net Depth (m)	Treatment Mass (g)	Release Time (hr)
1	97600	874000	5	477.46	0
2	97642	873973	5	477.46	24
3	97684	873946	5	477.46	48
4	97726	873918	5	477.46	72
5	97768	873891	5	477.46	96
6	97810	873864	5	477.46	120
7	97852	873837	5	477.46	144
8	97573	873958	5	477.46	168
9	97615	873931	5	477.46	192
10	97657	873904	5	477.46	216
11	97699	873876	5	477.46	240
12	97741	873849	5	477.46	264
13	97782	873822	5	477.46	288
14	97824	873795	5	477.46	312

3 RESULTS

3.1 Dispersion During Neap Tides, July 2020 (ID342)

A standard treatment of 14 100m pens, with a reduced net depth of 5 m and assuming 1 pen could be treated per day at a treatment concentration of 120 µg/L, resulted in a treatment mass per cage of azamethiphos of 477 g for, a daily (24-h) release of 0.477 kg and a total treatment release of 6.685 kg over 312 hours. The dispersion of the medicine during and following treatment from Run 001 is illustrated in Figure 10. After 60 minutes, as the first days treatments was discharged, a discrete patch of medicine is evident. The maximum concentration at this time was about 120 µg/L, due to the release of the fourth treatment. After 33 hours, as the last of the second days treatments was discharged, discrete patches of medicine from Day 2 are still evident, but the patches of medicine from the first day have rapidly dispersed and are already down to concentrations of the same order as the EQS (0.04 µg/L). The maximum concentration at this time was again about 120 µg/L, due to the release of the fourth treatment of the day.

The treatment schedule completed after 312 hours (13 days). At this stage, the medicine released on earlier days has already dispersed north-westwards in the prevailing flow through the Sound of Harris. It is noticeable that dispersion of the medicine does not happen in a gradual “diffusive” manner, but is largely driven by eddies and horizontal shear in the spatially-varying velocity field, which stretches and distorts the medicine patches and enhances dispersion. Following the final treatment at 312 hours, the final treatment patches were rapidly dispersed and concentrations rapidly fell away.

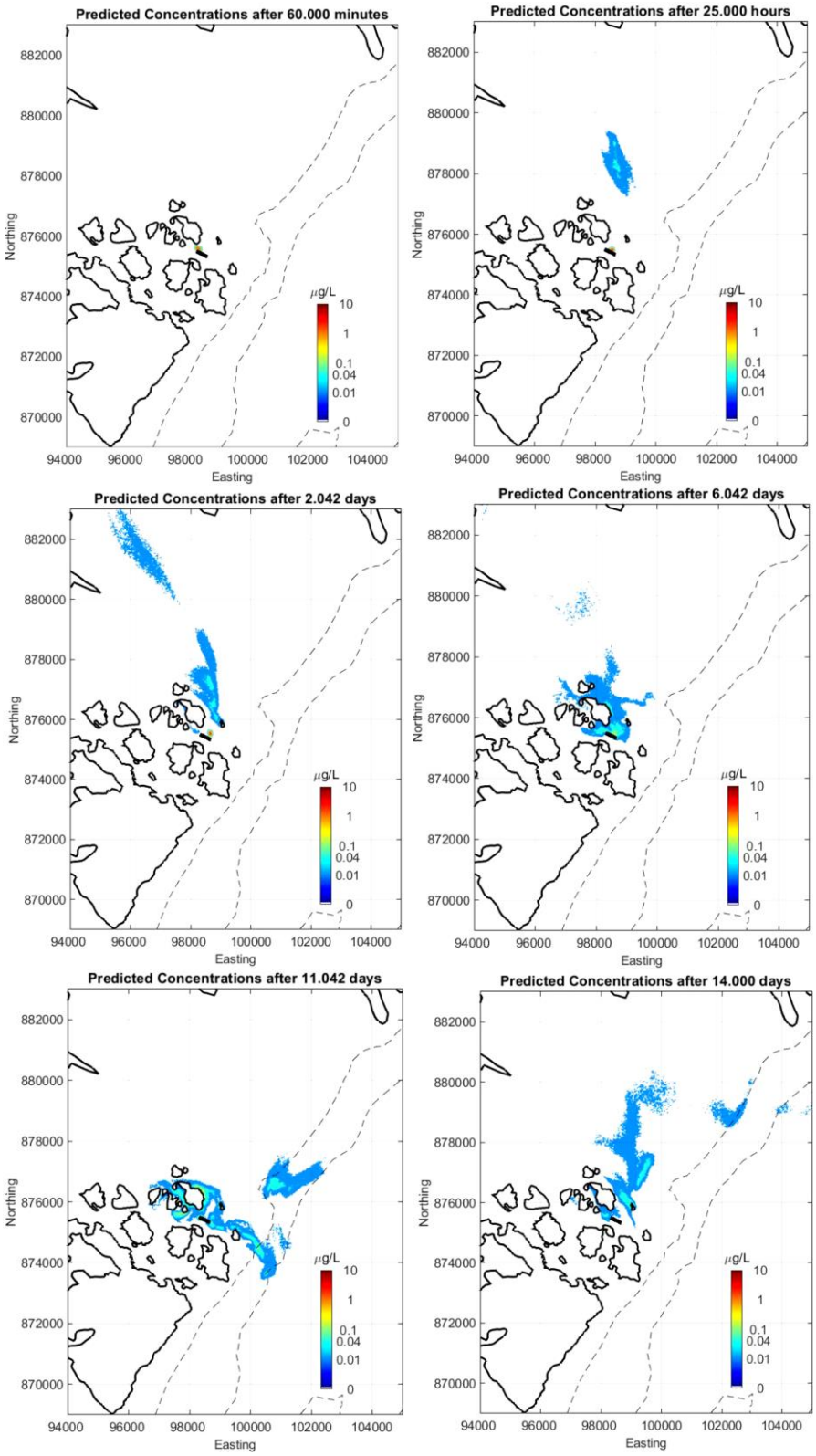

Figure 10. Predicted concentration fields for a dispersion simulation at neap tides after 1 hour (top left), 25 hours (top right), 49 hours (middle left), 145 hours (middle right), 265 hours (bottom left) and 336 hours (bottom right).

The time series of maximum concentration from the simulation is shown in Figure 11. The 12 peaks in concentration of 100 µg/L following each treatment event over the first 3 days are evident. Following the final treatment after 312 hours, the maximum concentration fell steadily away (Figure 11). With a default half-life of 134.4 h (5.6 days), the maximum concentration seventy-two hours after the final treatment (time = 384 hours) was below 0.1 µg/L, the maximum allowable concentration (MAC).

The area where the EQS of 0.04 µg/L was exceeded peaked at about 2.48 km^2 during treatment on days 11, but had fallen below 0.5 km^2 within 66h of the final treatment; by 72 h after the final treatment, the exceeded area was zero (Figure 11).

These results indicate that, with a horizontal diffusion coefficient of 0.1 m^2 s^{-1}, and a medicine half-life of 134.4 h, the environmental quality standards are comfortably achieved. In the following sections, the sensitivity of the model results to the medicine half-life, diffusion coefficients and tidal state are examined, with more realistic values being used in each case.

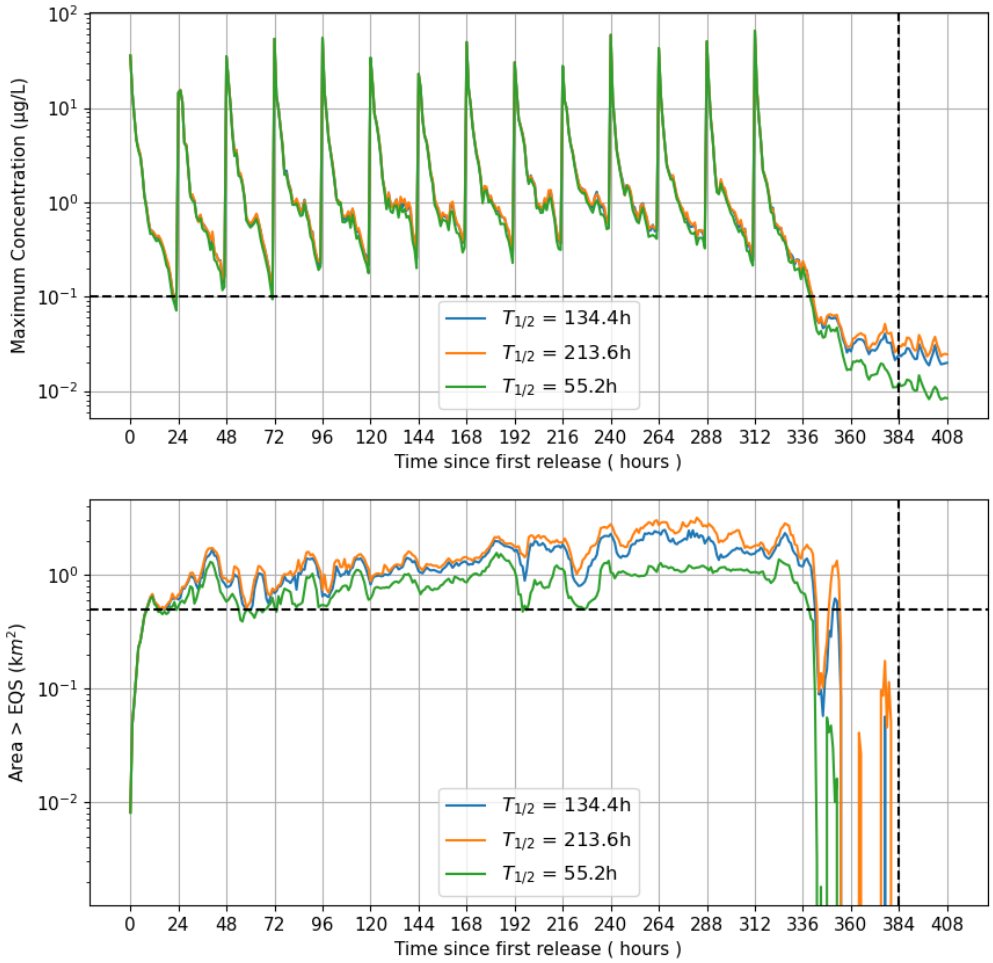

Figure 11. Time series of maximum concentration (top) and area exceeding the EQS (bottom) from the first set of model runs (Table 4). The model was run during neap tide with varying medicine half-life ($T_{1/2}$). The MAC and area limit 72 hours after the final treatment (Time = 384 h) of 0.1 µg/L and 0.5 km^2 are indicated by the horizontal dashed lines.

3.2 Sensitivity to Half-Life

The EQS was also achieved with a longer simulated medicine half-life of 213.6h (8.9) days, and was comfortably passed with a half-life of 55.2h (Figure 11). With the longer half-life, the area where the EQS of 0.04 µg/L is exceeded peaked at about 2.48 km^2 during treatments on day 11, but had fallen well below 0.5 km^2, for all simulated half-lives, within 66 hours of the final treatment (Figure 11). The area remained below 0.5 km^2 thereafter.

3.3 Sensitivity to Diffusion Coefficients

The model results were tested for sensitivity to the horizontal and vertical diffusion coefficients used. Although the diffusion coefficient used (K_H = 0.1 m^2 s^{-1}) is thought to be conservative, the diffusion coefficients estimated from individual transects through dye patches at Grey Horse Channel had a mean value of 0.094 m^2 s^{-1}. Simulations were therefore performed with lower and higher values of K_H, specifically K_H = 0.05 m^2 s^{-1} and K_H = 0.2 m^2 s^{-1} (Table 4).

The time series of maximum concentration and area exceeding the EQS are shown in Figure 12. The time series confirm that the MAC was not exceeded after 384 hours (72 hours after the final treatment) with either the lower or higher value of K_H. The area limit of 0.5 km^2 was comfortably met in all cases.

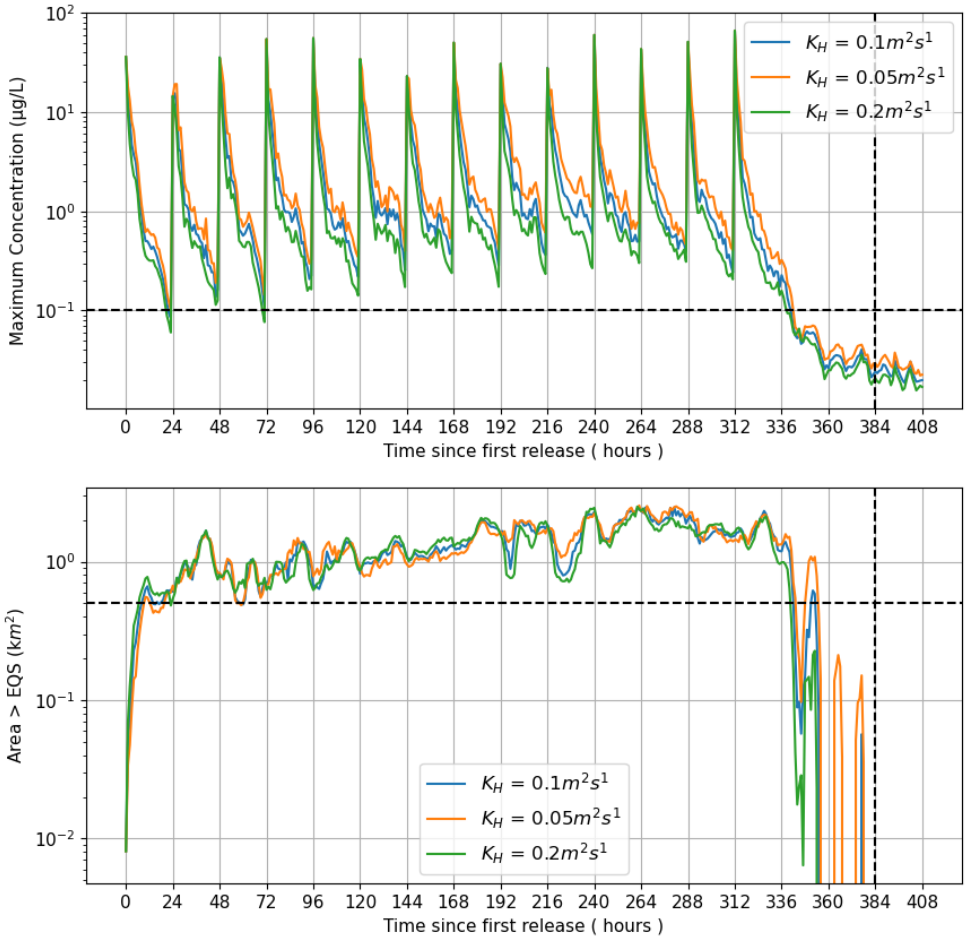

Figure 12. Time series of maximum concentration (top) and area exceeding the EQS (bottom) from the second set of model runs (Table 4). The model was run during neap tide with varying horizontal diffusion coefficient K_H. The MAC and area limit 72 hours after the final treatment (Time = 384 h) of 0.1 µg/L and 0.5 km^2 are indicated by the horizontal dashed lines.

Similarly, sensitivity to the vertical diffusion coefficient, K_V, was tested (Figure 13). The model is not particularly sensitive to the vertical diffusion rate, but increased vertical diffusion, likely in the presence of wind and/or waves, led to slightly lower peak concentrations and a smaller area where the EQS was exceeded.

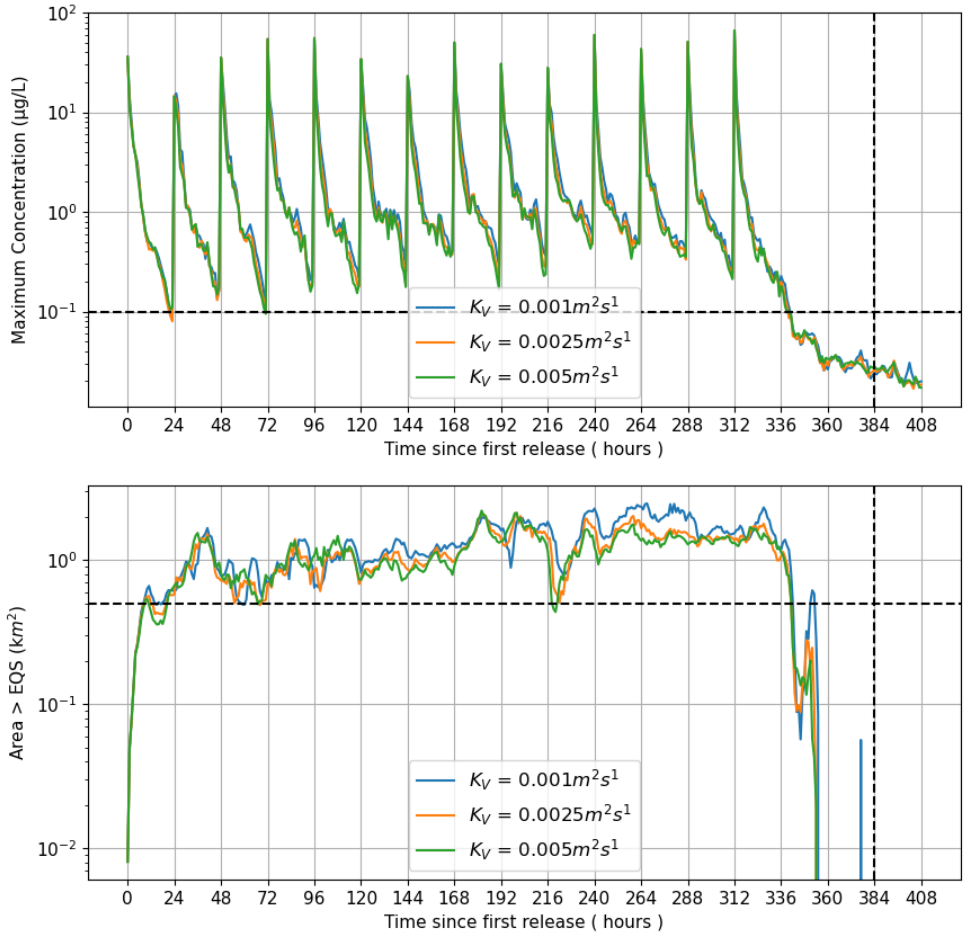

Figure 13. Time series of maximum concentration (top) and area exceeding the EQS (bottom) from the third set of model runs (Table 4). The model was run during neap tides with varying vertical diffusion coefficient K_V. The MAC and area limit 72 hours after the final treatment (Time = 384 h) of 0.1 µg/L and 0.5 km^2 are indicated by the horizontal dashed lines.

3.4 Sensitivity to Release Time

The baseline simulations were repeated with the time of the releases varied by up to ±6 hours, the purpose being to assess the influence, if any, of the state of the tide on subsequent dispersion. All time sensitivity variation simulations achieved the EQS comfortably (Figure 14).

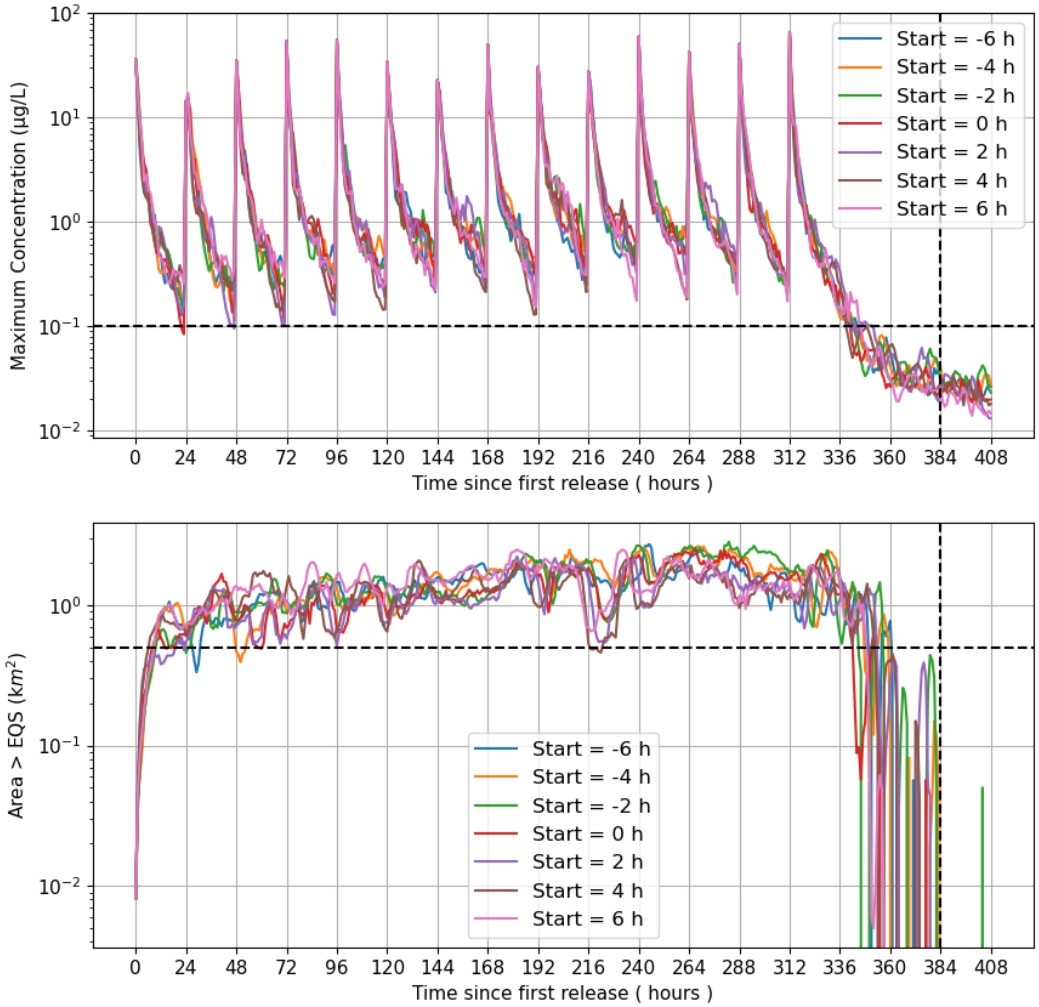

Figure 14. Time series of maximum concentration (top) and area exceeding the EQS (bottom) from the fourth set of model runs (Table 4). The model was run during neap tides with varying release times, relative to the baseline (Start = 0 h). The MAC and area limit 72 hours after the final treatment (Time = 384 h) of 0.1 µg/L and 0.5 km^2 are indicated by the horizontal dashed lines.

3.5 Dispersion during Spring Tides, June - July 2020 (ID342)

Dispersion simulations were carried out during modelled spring tides in later June to early July 2020 (Figure 6), repeating the main set carried out for neap tides (Table 4). The same treatment scenario of 1 treatment per day was simulated, with each treatment using 477g of azamethiphos. For all medicine half-lives and horizontal and vertical diffusion coefficients simulated, both the MAC and area EQS were comfortably achieved (Figure 15). Since treatment of the sites took almost two weeks, covering a full spring-neap cycle, there is not a significant difference between model results at springs and neaps.

Given the comfortable compliance with the MAC and EQS at spring tides, simulations investigating the effects of release times were not performed.

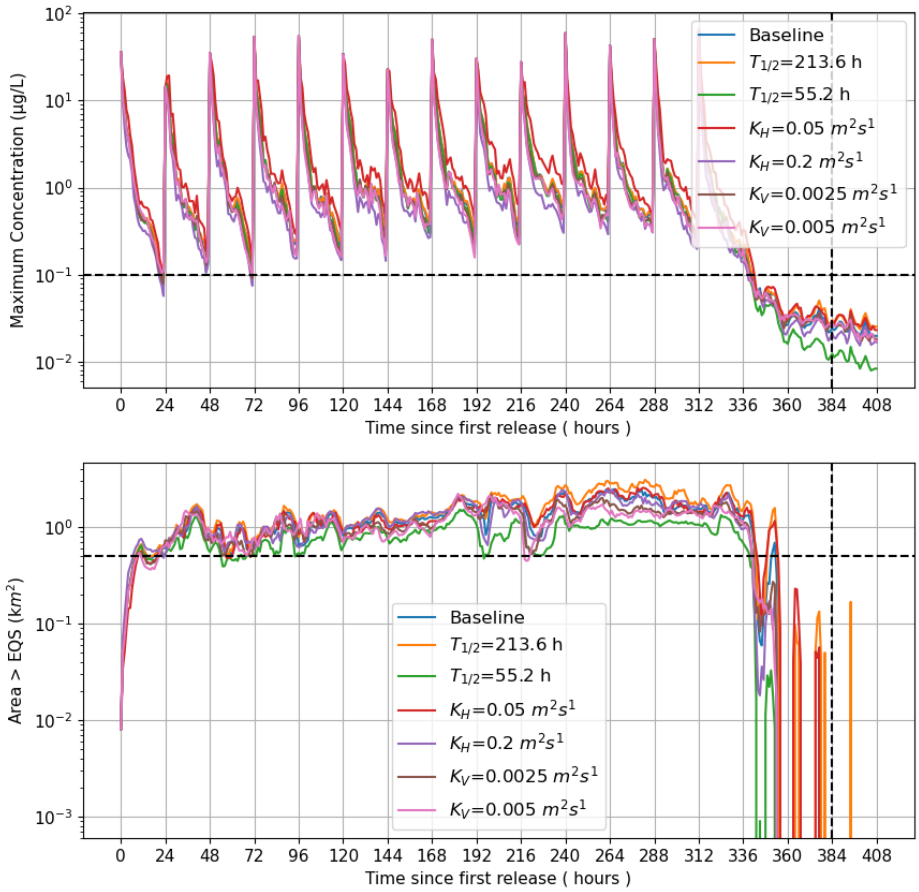

Figure 15. Time series of maximum concentration (top) and the area where concentrations exceeded the EQS (bottom) from the fifth set of model runs (Table 4). The model was run at spring tides with varying medicine half-life ($T_{1/2}$), horizontal diffusion coefficient (K_H) and vertical diffusion coefficient (K_V). The MAC and area limit 72 hours after the final treatment (Time = 384 h) of 0.1 µg/L and 0.5 km^2 are indicated by the horizontal dashed lines.

3.6 Dispersion during Neap tides July 2018 (ID210)

A further set of dispersion simulations during modelled neap tides from 20th June 2018 – 6th July 2018 (Figure 7), repeating the main set carried out for neap tides (Table 4). The same treatment scenario of 1 treatment per day was simulated, with each treatment using 477 g of azamethiphos. For all medicine half-lives, and horizontal and vertical diffusion coefficients simulated, both the MAC and area EQS were comfortably achieved, except for the conservative half-life of 8.9 days, the horizontal diffusivity of 0.05 m/s and a brief, very minor, exceedance of area for the baseline (Figure 16).

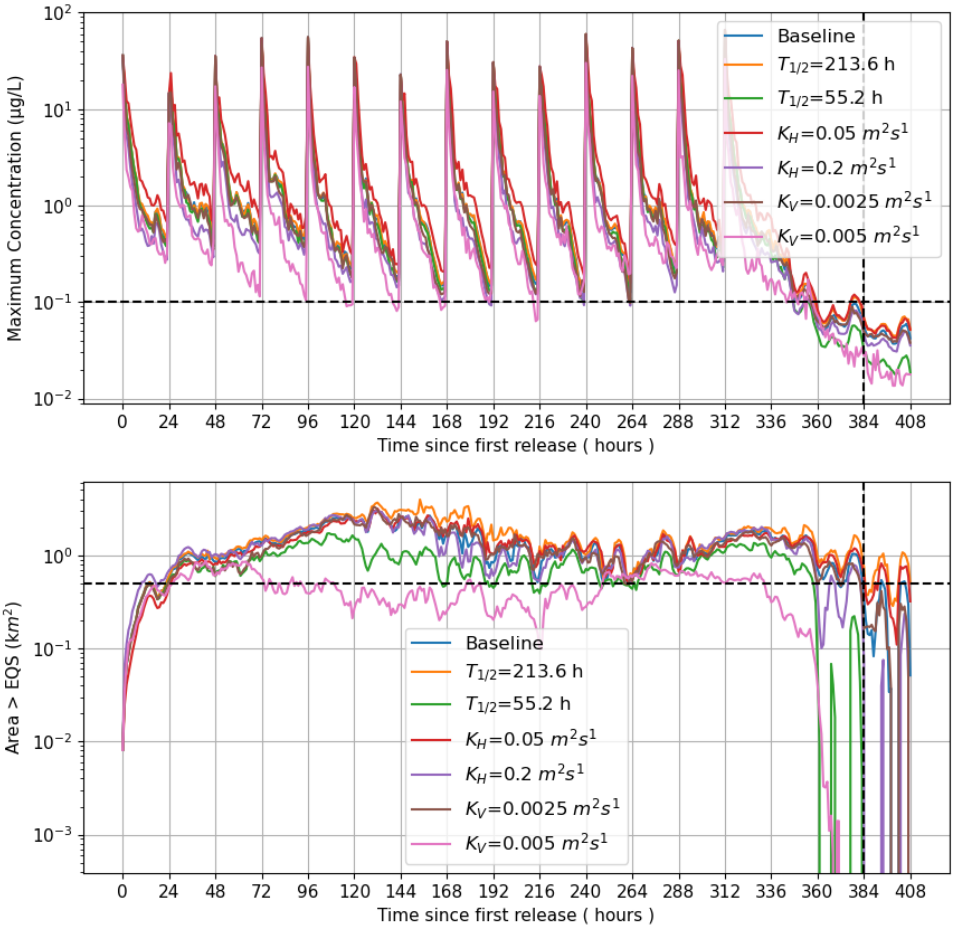

Figure 16. Time series of maximum concentration (top) and the area where concentrations exceeded the EQS (bottom) from the sixth set of model runs (Table 4). The model was run at neap tides in June 2020 with varying medicine half-life ($T_{1/2}$), horizontal diffusion coefficient (K_H) and vertical diffusion coefficient (K_V). The MAC and area limit 72 hours after the final treatment (Time = 384 h) of 0.1 µg/L and 0.5 km^2 are indicated by the horizontal dashed lines.

3.7 Cumulative Modelling

3.7.1 Grey Horse Channel and Grey Horse Channel Outer

Runs 1-13 described in Table 4 were repeated with simultaneous treatments made at the neighbouring Grey Horse Channel Outer site, simulations at Grey Horse Channel Outer start 48 hours later than Grey Horse Channel due to Grey Horse Channel Outer having 12 pens.

In total, therefore, 1.165 kg of azamethiphos was discharged at each simultaneous release (0.477 kg at Grey Horse Channel and 0.688 kg at Grey Horse Channel Outer). 1.165 kg was the total daily release at both sites during simultaneous treatments.

The conservative half-life simulation of 8.9 days fails the area EQS (Figure 17), there are multiple small failures of EQS for the time sensitivity runs (Figure 18), and the lower horizontal diffusivity simulation of 0.05 m^2s^1 also fails the area and concentration EQS (Figure 19) The flow fields used are considered conservative (see Annex A) and this cumulative modelling represents an unlikely treatment scenario.

A selection of results are presented below. Note that since two sites are modelled, an area EQS of 1.0 km^2 is applied, since the allowable exceedance area of 0.5 km^2 applies separately to both sites. The MAC remains unaffected by the simultaneous treatment regime at 100 µg/L.

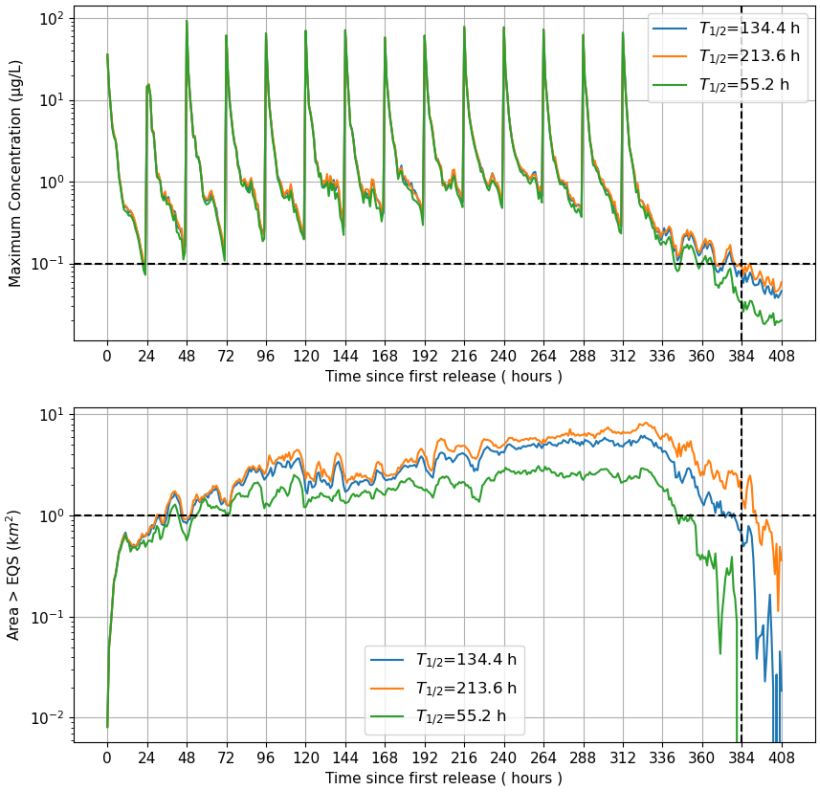

Figure 17. Time series of maximum concentration (top) and area exceeding the EQS (bottom) from simulations of simultaneous treatments at Grey Horse Channel Outer and Grey Horse Channel sites during neap tides in July 2018 (Runs 1 – 3, Table 4). The model was run with varying medicine half-life ($T_{1/2}$). The MAC and area limit 72 hours after the final treatment (Time = 384 h, vertical dashed line) of 0.1 µg/L and 1.0 km^2 are indicated by the horizontal dashed lines.

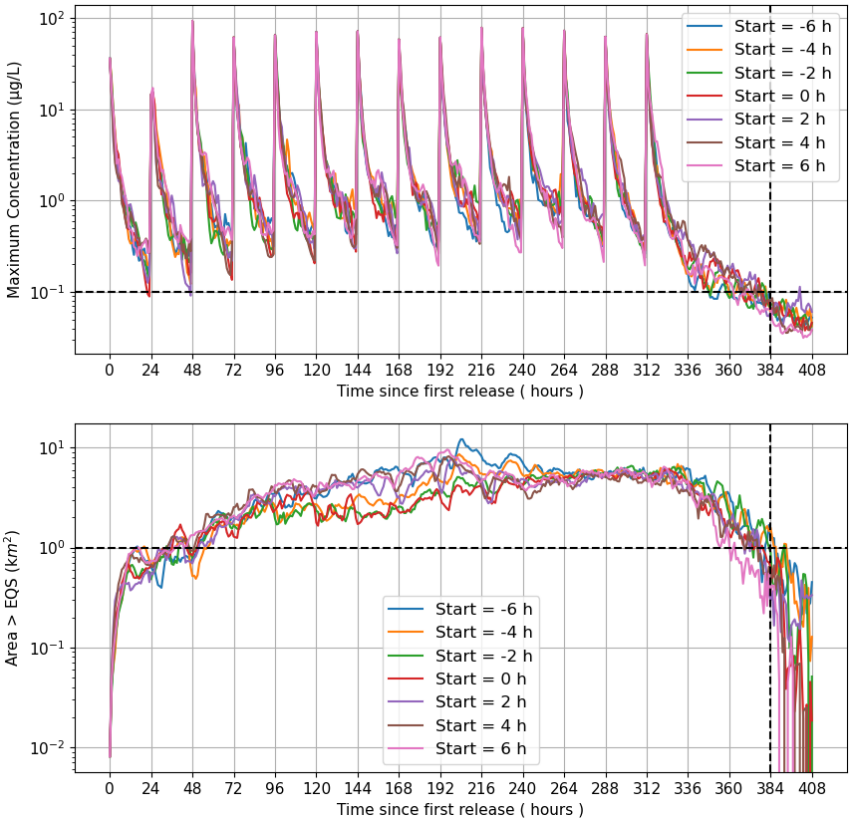

Figure 18. Time series of maximum concentration (top) and area exceeding the EQS (bottom) for simultaneous treatments at Grey Horse Channel Outer and Grey Horse Channel from the third set of model runs (Table 4). The model was run during neap tides in July 2018 with varying release times, relative to the baseline (Start = 0 h). The MAC and area limit 72 hours after the final treatment (Time = 384 h) of 0.1 µg/L and 1.0 km^2 (2 x 0.5 km^2) are indicated by the horizontal dashed lines.

3.7.2 Grey Horse Chanel, Grey Horse Channel Outer and Groatay Simultaneous Treatments

Runs 1-13 described in Table 4 were repeated with simultaneous treatments made at the neighbouring Groatay site, in addition to the existing simulations at Grey Horse Channel and Grey Horse Channel Outer. Simulations at Groatay are contemporaneous with Grey Horse Channel.

In total, therefore, 1.642 kg of azamethiphos was discharged at each simultaneous release of the 3 sites (0.477 kg at Grey Horse Channel and Groatay and 0.688 kg at Grey Horse Channel Outer). 1.642 kg was the daily release at all 3 sites combined during simultaneous releases.

The lower horizontal diffusivity simulation of 0.05 m^{2}s^1 fails the area and concentration EQS (Figure 19), the conservative half-life simulations of 8.9 and 5.6 days fail the area EQS (Figure 20), the and there are multiple small failures of EQS for the time sensitivity runs (Figure 21). The flow fields used are considered conservative and this cumulative modelling represents an unlikely treatment scenario.

Note that since three sites are modelled, an area EQS of 1.5 km^2 is applied, since the allowable exceedance area of 0.5 km^2 applies separately to each site. The MAC remains unaffected by the simultaneous treatment regime at 100 µg L^{-1}.

The time sensitivity runs which fail to comply with environmental quality standards are considered an extremely unlikely treatment scenario requiring synchronised prolonged treatments across 3 separate sites.

Figure 22 shows results from simultaneous treatments at both sites at a 1 pen per day treatment schedule for a release during neap tides in July 2018. The times series for different medicine half-lives times are shown.

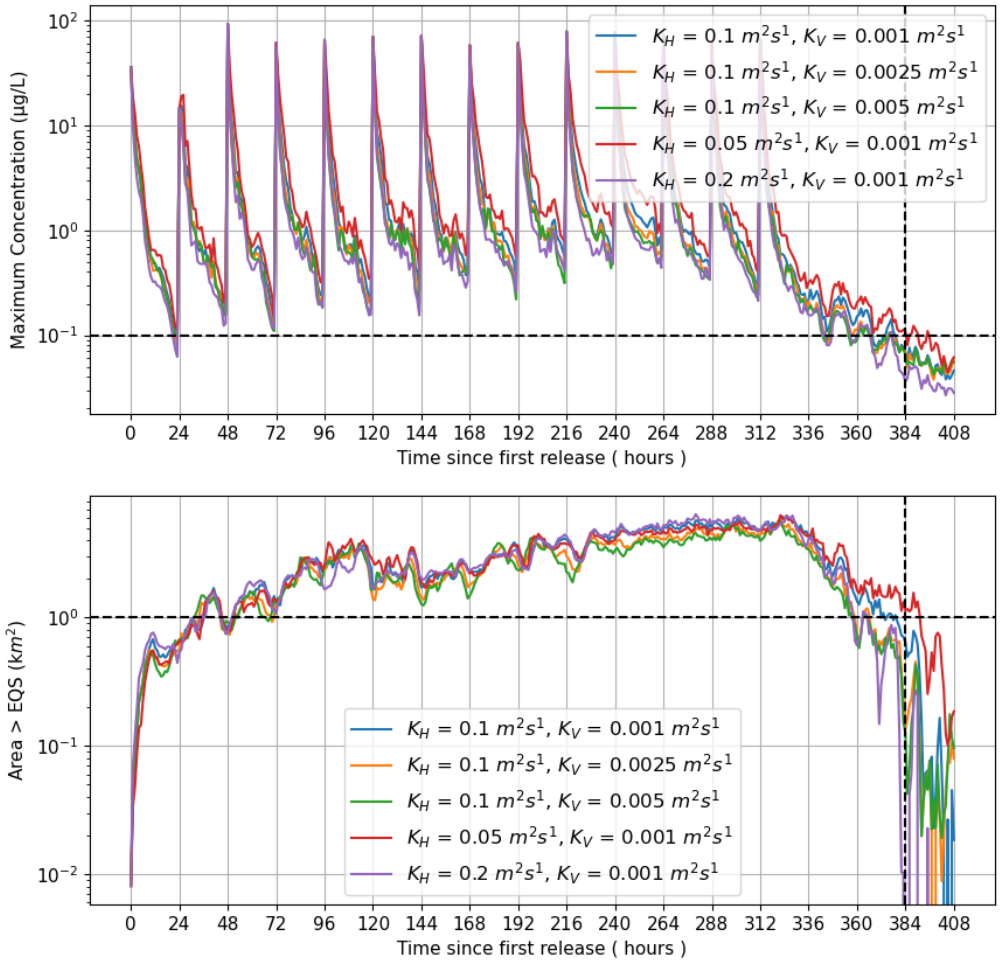

Figure 19. Time series of maximum concentration (top) and area exceeding the EQS (bottom) for simultaneous treatments at Grey Horse Channel and Grey Horse Channel Outer from the 4th and 5th set of model runs (Table 4). The model was run during neap tides in July 2018 with varying horizontal (K_H) and vertical (K_V) diffusivity. The MAC and area limit 72 hours after the final treatment (Time = 384 h) of 0.1 µg/L and 1.0 km^2 (2 x 0.5 km^2) are indicated by the horizontal dashed lines.

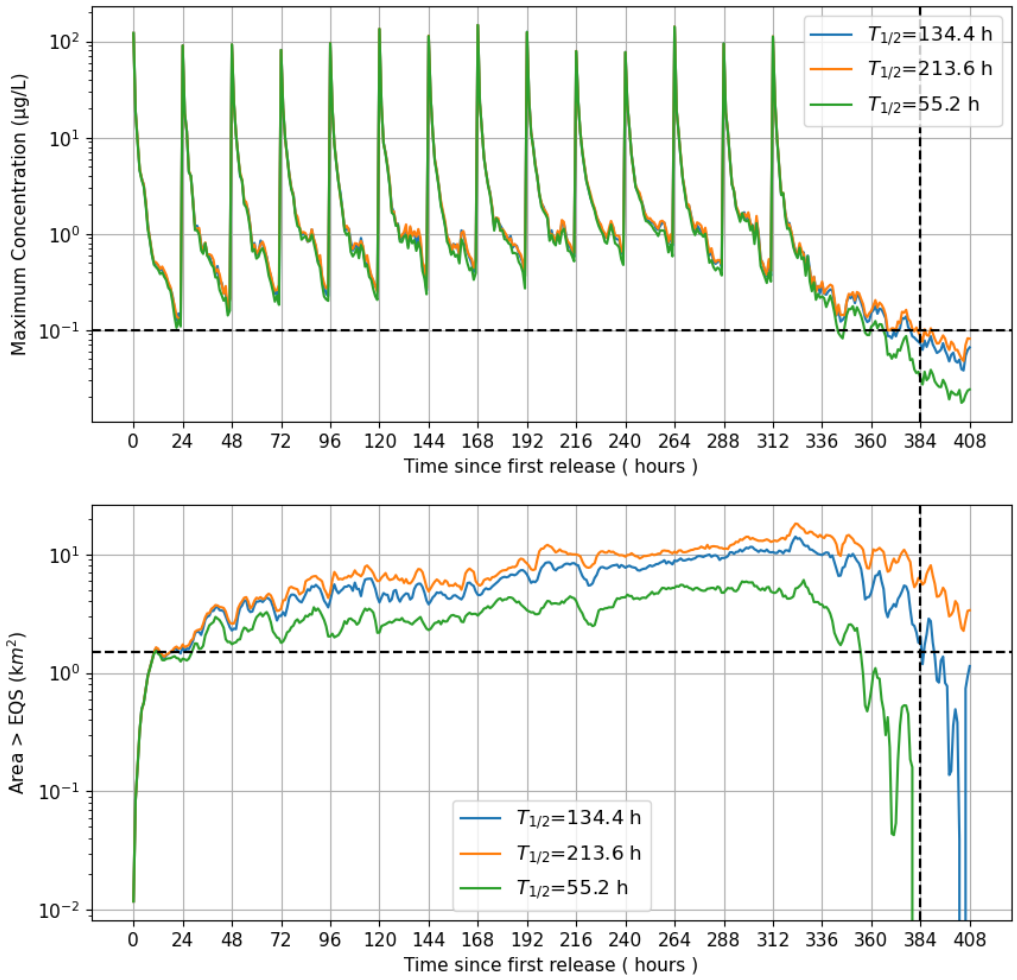

Figure 20. Time series of maximum concentration (top) and area exceeding the EQS (bottom) from simulations of simultaneous treatments at Grey Horse Channel, Grey Horse Channel Outer and Groatay sites during neap tides in 2020 (Runs 1 – 3, Table 4). The model was run with varying medicine half-life ($T_{1/2}$). The MAC and area limit 72 hours after the final treatment (Time = 384 h, vertical dashed line) of 0.1 µg/L and 1.5 km^2 are indicated by the horizontal dashed lines.

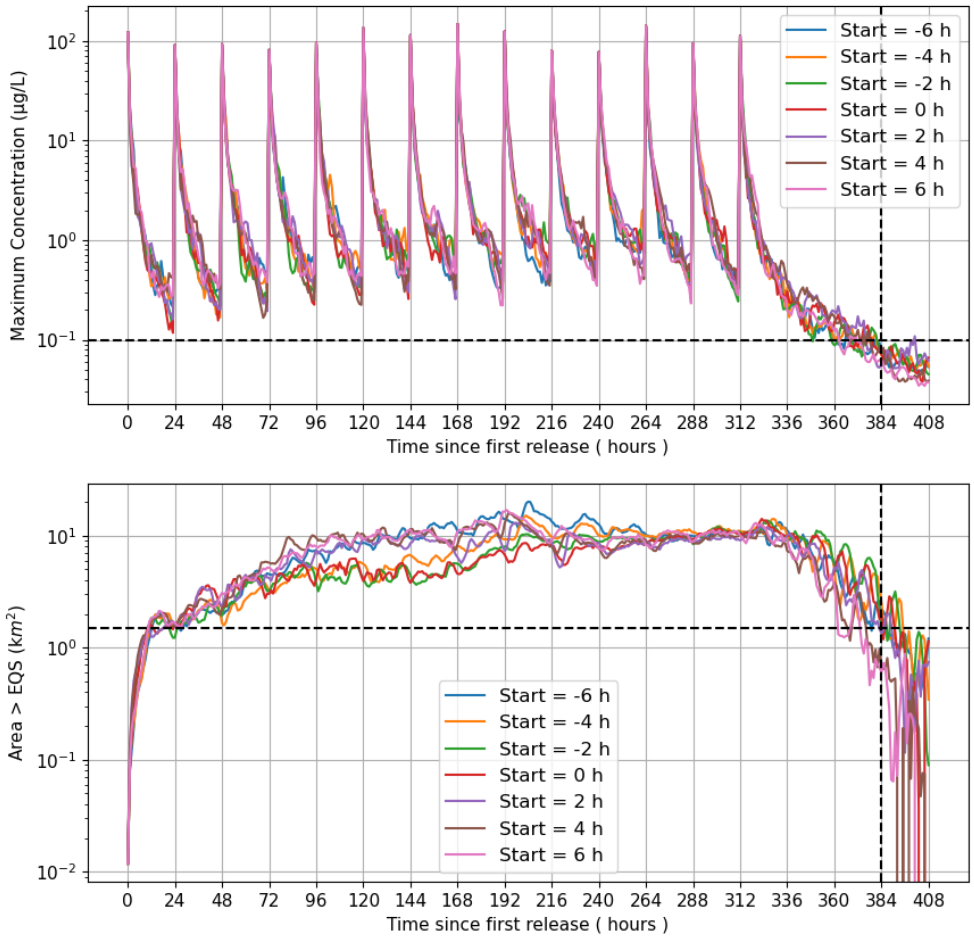

Figure 21. Time series of maximum concentration (top) and area exceeding the EQS (bottom) for simultaneous treatments at Grey Hose Channel Outer, Grey Horse Channel and Groatay. The model was run during neap tides in July 2018 with varying start times. The MAC and area limits for three sites 72 hours after the final treatment (Time = 120 h) of 0.1 µg/L and 1.5 km^2 respectively are indicated by the horizontal dashed lines.

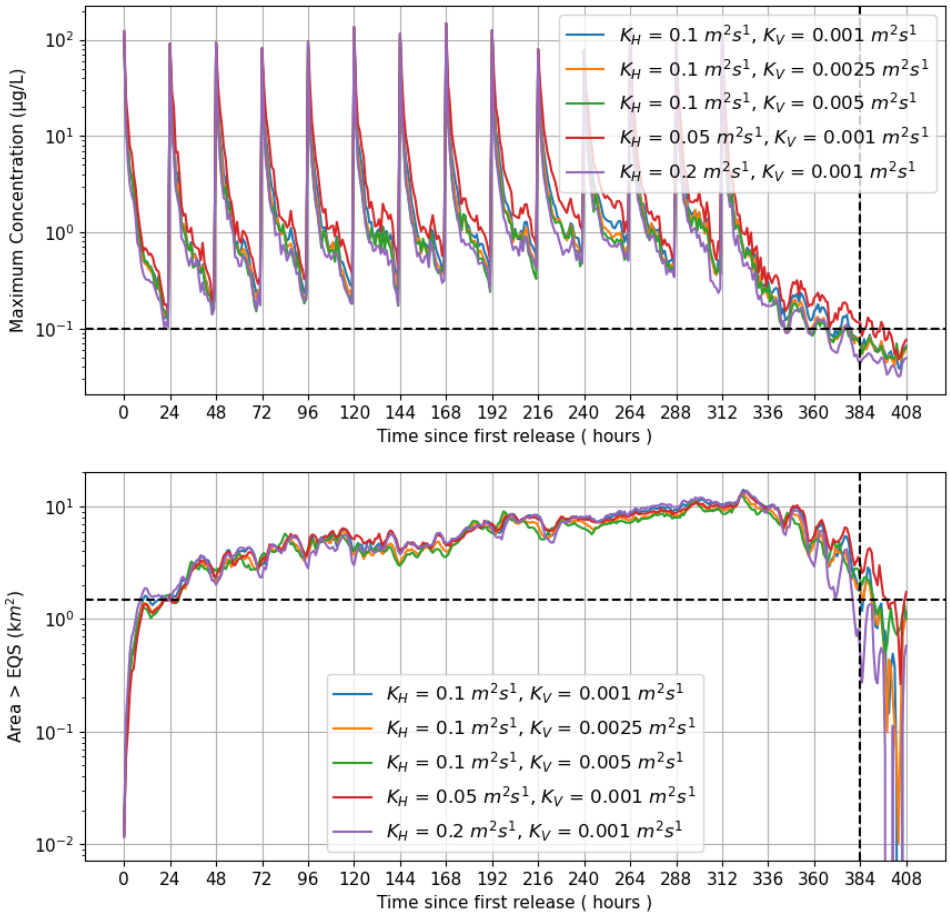

Figure 22. Time series of maximum concentration (top) and area exceeding the EQS (bottom) for simultaneous treatments at Grey Horse Channel Outer, Grey Horse Channel and Groatay from the 4th and 5th set of model runs (Table 4). The model was run during neap tides in July 2018 with varying horizontal (K_H) and vertical (K_V) diffusivity. The MAC and area limit 72 hours after the final treatment (Time = 384 h) of 0.1 µg/L and 1.5 km^2 (3 x 0.5 km^2) are indicated by the horizontal dashed lines.

4 SUMMARY AND CONCLUSIONS

A total of 52 dispersion simulations (including 26 cumulative) have been performed to assess whether bath treatments at Grey Horse Channel salmon farm will comply with pertinent environmental quality standards. A realistic treatment regime, with 1 cage treatments a day was simulated. Each pen required 477 g of azamethiphos for treatment, resulting in a daily release of 0.477 kg and a total discharge over 4 days of 6.68 kg. Simulations were performed separately for modelled neap and spring tides, and the sensitivity of the results to key model parameters was tested. Results are summarised in Table 7.

Table 7.Summary of Results

SITE DETAILS			
Site Name:		Grey Horse Channel	
Site location:		Sound of Harris	
Peak biomass (T):		1,750	
CAGE DETAILS			
Number of cages:		14	
Cage dimensions:		100m Circumference	
Working Depth (m):		12	
Cage group configuration:		2 x 7, 60m matrix	
HYDROGRAPHIC SUMMARY			
	Grey Horse Channel	**Jun-Aug 2020**	**Mar-Jul 2018**
Surface Currents	Mean Speed (m/s)	0.182	0.108
	Residual Speed (m/s)	0.037	0.005
	Residual Direction (°G)	108	008
	Tidal Amplitude Parallel (m/s)	0.278	0.175
	Tidal Amplitude Normal (m/s)	0.091	0.045
	Major Axis (°G)	130	310
BATH TREATMENTS			
Recommended consent mass - 3hr Azamethiphos (g)		477	
Recommended consent mass - 24hr Azamethiphos (g)		477	

The model results confirmed that the treatment scenario proposed, with a daily release of no more than 0.477 kg, should consistently comply with the EQS. The peak concentration during the baseline simulation after 384 hours (72 hours after the final treatment) was less than 0.1 µg/L, the maximum allowable concentration, and the area where concentrations exceeded the EQS of 0.04 µg/L was substantially less than the allowable 0.5 km^2. In almost all simulations performed, including some sensitivity testing, the EQS criteria were met. Simulations over two different neap tides from 2018 and 2020 demonstrated that the modelled treatment regime complied with the relevant EQS. For the simulation during spring tides, greater dispersion meant that the EQS were met. The minor exceedance of EQS observed can be explained by the conservative nature of the modelled flows as demonstrated in Annex A. Therefore, we

believe that the requested daily quantity of 0.477 kg of azamethiphos can be safely discharged without breaching the EQS.

The 24-hour mass is larger than the amount predicted by the standard bath model, but the latter is known to be highly conservative, because it does not account for horizontal shearing and dispersion of medicine patches due to spatially-varying current fields, processes which are known to significantly influence dispersion over times scales greater than a few hours (e.g. Okubo, 1971; Edwards, 2015), as illustrated in Figure 10.

5 REFERENCES

Allen, C.M., 1982. Numerical simulation of contaminant dispersion in estuary flows. Proc. Royal. Soc. London (A), 381, 179–194.

Brickman, D., Ådlandsvik, B., Thygesen, U.H., Parada, C., Rose, K., Hermann, A.J. and Edwards, K., 2009. Particle Tracking. In: Manual of Recommended Practices for Modelling Physical – Biological Interactions during Fish Early Life, pp. 27 – 42. Ed. by E. W. North, A. Gallego, and P. Petitgas. ICES Cooperative Research Report No. 295. 111 pp.

Chen, C., Lui, H., Beardsley, R.C., 2003. An unstructured, finite-volume, three-dimensional, primitive equation ocean model: Application to coastal ocean and estuaries, J. Atmos. Oceanic Technol., 20, 159–186.

Dale. A., Allen. C., Venables. E., Beaton. J. and Aleynik. D. (2020). Dye tracer dispersion studies in support of bath treatment models for fish farms (2020). A study commissioned by the Scottish Aquaculture Research Forum (SARF). http://www.sarf.org.uk/SARFSP012.pdf

Edwards, A., 2015. A note on dispersion in West Scottish coastal waters. A Report for Benchmark Animal Health. September 2015, 55pp.

Gillibrand, P.A., 2020. Unptrack User Guide. Mowi Scotland Ltd., June 2020.

Gillibrand, P.A., B. Siemering, P.I. Miller and K. Davidson, 2016. Individual-Based Modelling of the Development and Transport of a Karenia mikimotoi Bloom on the North-West European Continental Shelf. Harmful Algae, DOI: 10.1016/j.hal.2015.11.011

Gillibrand, P.A., Walters, R.A., and McIlvenny, J., 2016. Numerical simulations of the effects of a tidal turbine array on near-bed velocity and local bed shear stress. *Energies*, vol 9, no. 10, pp. 852. DOI: 10.3390/en9100852

Gillibrand, P.A. and K.J. Willis, 2007. Dispersal of Sea Lice Larvae from Salmon Farms: A Model Study of the Influence of Environmental Conditions and Larval Behaviour. Aquatic Biology, 1, 73-75.

Hunter J.R., Craig, P.D., Phillips, H.E. 1993. On the use of random walk models with spatially variable diffusivity. J Comput. Phys., 106:366–376

Lewis, R. 1997. Dispersion in Estuaries and Coastal Waters. John Wiley and Sons, 332 pp.

McIlvenny, J. , Tamsett, D., Gillibrand, P.A. and Goddijn-Murphy, L., 2016. Sediment Dynamics in a Tidally Energetic Channel: The Inner Sound, Northern Scotland. Journal of Marine Science and Engineering, 4, 31; doi:10.3390/jmse4020031

MS 2016. The Scottish Shelf Model. Marine Scotland. http://marine.gov.scot/themes/scottish-shelf-model

Okubo, A., 1971. Oceanic diffusion diagrams. Deep-Sea Research, 18, 789 – 802.

Proctor, R., R.A. Flather and A.J. Elliott, 1994. Modelling tides and surface drift in the Arabian Gulf---application to the Gulf oil spill. Continental Shelf Research, 14, 531-545.

Ross, O.N., Sharples, J., 2004. Recipe for 1-D Lagrangian particle tracking models in space-varying diffusivity. Limnology and Oceanography: Methods, 2, 289-302.

SEPA, 2019. Aquacultre Modelling. Regulatory modelling guidance for the aquaculture sector. Scottish Environment Protection Agency, Air and Marine Modelling Unit, June 2019, 68pp.

SEPA, 2020. Aquaculture Modelling Screening and Risk Identification Report: Loch Hourn (HNW1). Scottish Environment Protection Agency, February 2020, 28pp.

Visser, A.W., 1997. Using random walk models to simulate the vertical distribution of particles in a turbulent water column. Mar. Ecol. Prog. Ser., 158, 275-281.

Walters, R.A.; Casulli, V., 1998. A robust, finite element model for hydrostatic surface water flows. Comm. Num. Methods Eng., 14, 931–940.

Willis, K.J, Gillibrand, P.A., Cromey, C.J. and Black, K.D., 2005. Sea lice treatments on salmon farms have no adverse effect on zooplankton communities: A case study. *Marine Pollution Bulletin*, 50, 806 – 816.

ANNEX A. HYRODYNAMIC MODEL DESCRIPTION

A.1 Model Description

The hydrodynamic model used in this study was RiCOM (River and Coastal Ocean Model), a general-purpose hydrodynamics and transport model, which solves the standard Reynolds-averaged Navier-Stokes equation (RANS) and the incompressibility condition, applying the hydrostatic and Boussinesq approximations. It has been tested on a variety of benchmarks against both analytical and experimental data sets (e.g. Walters and Casulli 1998; Walters 2005a, b). The model has been previously used to investigate the inundation risk from tsunamis and storm surge on the New Zealand coastline (Walters 2005a; Gillibrand et al. 2011; Lane et al. 2011), to study tidal currents in high energy tidal environments (Walters et al. 2010) and, more recently, to study tidal energy resource (Plew and Stevens 2013; Walters et al. 2013; Walters 2016) and the effects of energy extraction on the ambient environment (McIlvenny et al. 2016; Gillibrand et al. 2016).

The basic equations considered here are the three-dimensional (3D) shallow water equations, derived from the Reynolds-averaged Navier-Stokes equations by using the hydrostatic assumption and the Boussinesq approximation. The continuity equation for incompressible flows is:

$$\nabla \cdot u + \frac{\partial w}{\partial z} = 0 \tag{A1}$$

where **u**(x,y,z,t) is the horizontal velocity vector, w(x,y,z,t) is the vertical velocity, ∇ is the horizontal gradient operator, and z is the vertical coordinate. The momentum equation in non-conservative form is given by [25]:

$$\frac{Du}{Dt} + f\hat{z} \times u + \frac{1}{\rho_0}\nabla p - \frac{\partial}{\partial z}\left(A_V \frac{\partial u}{\partial z}\right) - \nabla \cdot (A_h \nabla u) + F = 0 \tag{A2}$$

where t is time; f(x,y) is the Coriolis parameter; $\hat{\mathbf{z}}$ is the upward unit vector; p(x,y,z,t) is pressure; ρ_0 is a reference density; A_V(x,y,z,t) and A_h(x,y,z,t) are the vertical and horizontal eddy viscosities respectively; **F** represents body forces including form drag from obstacles in the flow; and x, y are the horizontal coordinates aligned to the east and north respectively.

The free surface equation is formed by vertically integrating the continuity equation and applying the kinematic free surface and bottom boundary conditions:

$$\frac{\partial \eta}{\partial t} - \nabla \cdot \left(\int_{\square}^{\eta} u dz\right) = 0 \tag{A3}$$

where h is the water depth relative to the mean level of the sea.

The model was run in three-dimensional mode, with 11 vertical sigma levels at σ = [0, -0.1, -0.2, -0.3, -0.4, -0.5, -0.6, -0.7, -0.8, -0.9, -1.0]. Velocities and scalar properties are calculated mid-layer.

Frictional stress, $\boldsymbol{\tau}_b$, was applied at the seabed as a quadratic function of velocity:

$$\tau_b = \rho C_D U_b |U_b| \tag{A4}$$

where ρ = 1025 kg m^{-3} is the water density. The velocity, U_b, is either the velocity at the lowest sigma layer if the model is run in 3D or the depth-averaged velocity if run in 2D. The drag coefficient, C_D, can be either a constant or calculated from the bed roughness length scale, z_0, using:

$$C_D = \left(\frac{\kappa}{\ln\left((z_b+z_0)/z_0\right)}\right)^2 \quad \text{(A5)}$$

where κ=0.4 is von Karman's constant, and z_b is the height above the bed of the lowest velocity point.

Wind forcing was applied as a surface stress calculated from hourly wind speed and direction. Wind stress was calculated from the wind velocity by a standard quadratic relation:

$$\tau_x = \rho_a C_S u W \quad \text{(A6a)}$$
$$\tau_y = \rho_a C_S v W \quad \text{(A6b)}$$

where (u,v) are the East and North components of wind velocity respectively, W is the wind speed ($W = [u^2+v^2]^{½}$), ρ_a is the density of air, and the surface drag coefficient C_S is calculated following Wu (1982).

The equations are discretized on an unstructured grid of triangular elements which permits greater resolution of complex coastlines. The momentum and free surface equations are solved using semi-implicit techniques to optimize solution time and avoid the CFL stability constraint (Walters 2016). The material derivative in (2) is discretized using semi-Lagrangian methods to remove stability constraints on advection (Casulli, 1987; Walters et al. 2008). The Coriolis term is solved using a 3rd order Adams-Bashforth method (Walters et al. 2009). Full details of the model discretization and solution methods can be found in Walters et al. (2013) and Walters (2016). The solution methods provide a fast, accurate and robust code that runs efficiently on multi-core desktop workstations with shared memory using OpenMP. Full details of the model discretization and solution methods, including the basis of the application to tidal energy, are given by Walters et al. (2013) and Walters (2016).

A.2 Configuration and Boundary Forcing for Cheesebay, North Uist

The RiCOM model has previously been calibrated against sea level and current meter data from the north of Scotland (Gillibrand et al. 2017). For the current study, the model was further calibrated against hydrographic data collected in the region of the farm site in 2018. The data are described in the relevant hydrographic reports. In March 2018, an Acoustic Doppler Current Profiler (ADCPs) was deployed close to the Grey Horse Channel farm site until July 2018. A further deployment were made from June - August 2020. In all, over 196 days of current data were used in this application. ADCP deployments provided both current velocity and seabed pressure data, which were used to calibrate and validate modelled velocity and sea surface height. The model was calibrated initially against data from 13 March – 10 July 2018, then validated against the data from both 9 June– 26 August 2020.

For each simulation, the model was "spun-up" for three days with boundary forcing ramped up from zero over a period of 48 hours. The model state at the end of the 72-hour spin-up period was stored, and the main simulations "hot-started" from this state.

The following main simulations were performed, corresponding with the dates of the ADCP deployments:

1. Calibration: 13th March – 10th July 2018 (ADCP deployment ID210)
2. Validation: 9th June – 26th August 2020 (ADCP deployment ID342)

[Note that the dates above refer to the main simulations and that the spin-up simulations ran for three days prior to the start dates given above.]

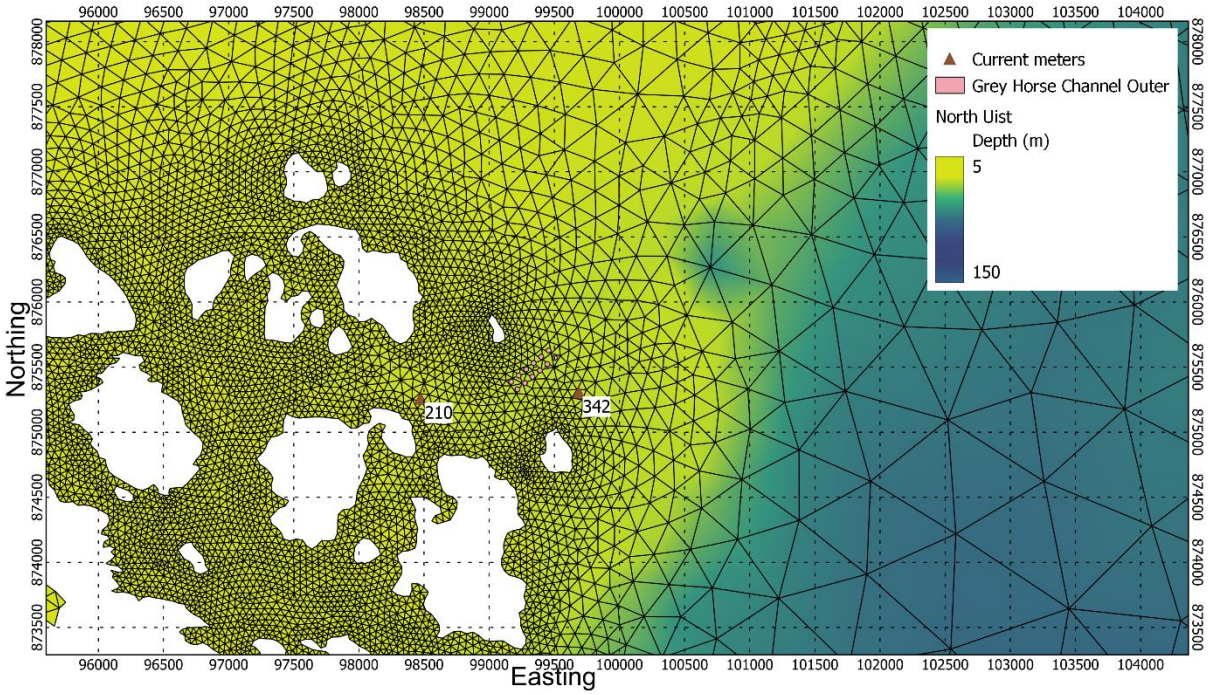

Figure A.1. Locations of the ADCP deployments relative to the 12 pens at the site.

Model performance is assessed using three metrics: the mean absolute error (MAE), the root-mean-square error (RMSE) and the model skill (d_2). The first two are standard measures of model accuracy; the third, d_2, is taken from Willmott et al. (1985) and lies in the range $0 \leq d_2 \leq 1$, with $d_2 = 0$ implying zero model skill and $d_2 = 1$ indicating perfect skill.

A.3.1 Calibration, March – July 2018

The calibration used observed depth and current velocity from the ADCP location to compare with modelled sea surface height (SSH) and velocity (ADCP deployment ID210). The model was calibrated by varying the value of the drag coefficient, C_D, in Equation A4, which determines the frictional effect of the seabed on the flow. Simulations were performed with a range of values of C_D, varying over the range $0.002 \leq C_D \leq 0.02$. After a number of simulations, a final parameter set was selected (Table A.).

Table A.1. Parameter values chosen for the RiCOM model during the calibration simulations.

Parameter Description	Value
Drag coefficient, C_D	0.018
Number of vertical levels	1
Model time step (s)	72.0

The results of the calibration exercise are presented in Figures A.2 – A.5 and Table A.A.2. At the ADCP location, the sea surface height was reasonably accurately modelled, with model skill of 0.99. The mean absolute error (MAE) and root-mean-square error (RMSE) values of 0.15 m and 0.18 m respectively are about 3% and 3.6% of the spring tide range respectively.

North and east components of velocity at the ADCP location were satisfactorily reproduced by the model, with values of the model skill, d_2, of 0.96 and 0.85 respectively for both (Figure A.3, Table A.2). The model slightly underpredicted the magnitude of the strongest observed currents (Figures A.4 and A.5), with values of MAE and RMSE being in the range 3 – 8 cm s^{-1} (Table A.3). This underprediction is unsurprising, with the model showing more spatially-smoothed currents than occur in reality, and provides a degree of conservatism in the following dispersion modelling. The scatter plots and histograms shown in Figures A.4 and A.5 demonstrate that the modelled currents were broadly of the same speed and direction as the observed data.

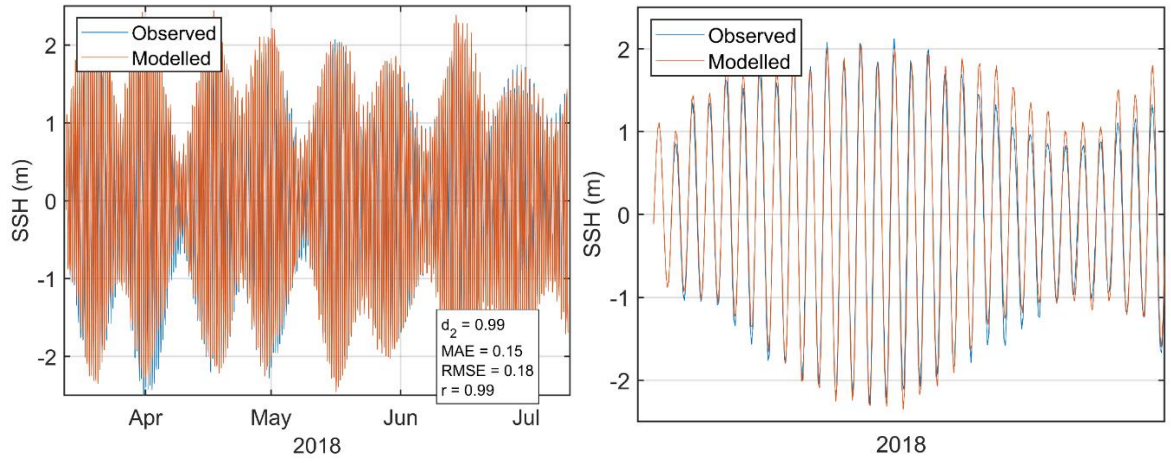

Figure A.2. Comparison between observed and modelled sea surface height from March - July 2018 (ADCP deployment ID210) using model parameter values from Table A.. Both the full record (left) and a subset of 15 days (right) are shown. Observed data are in blue, model results in red.

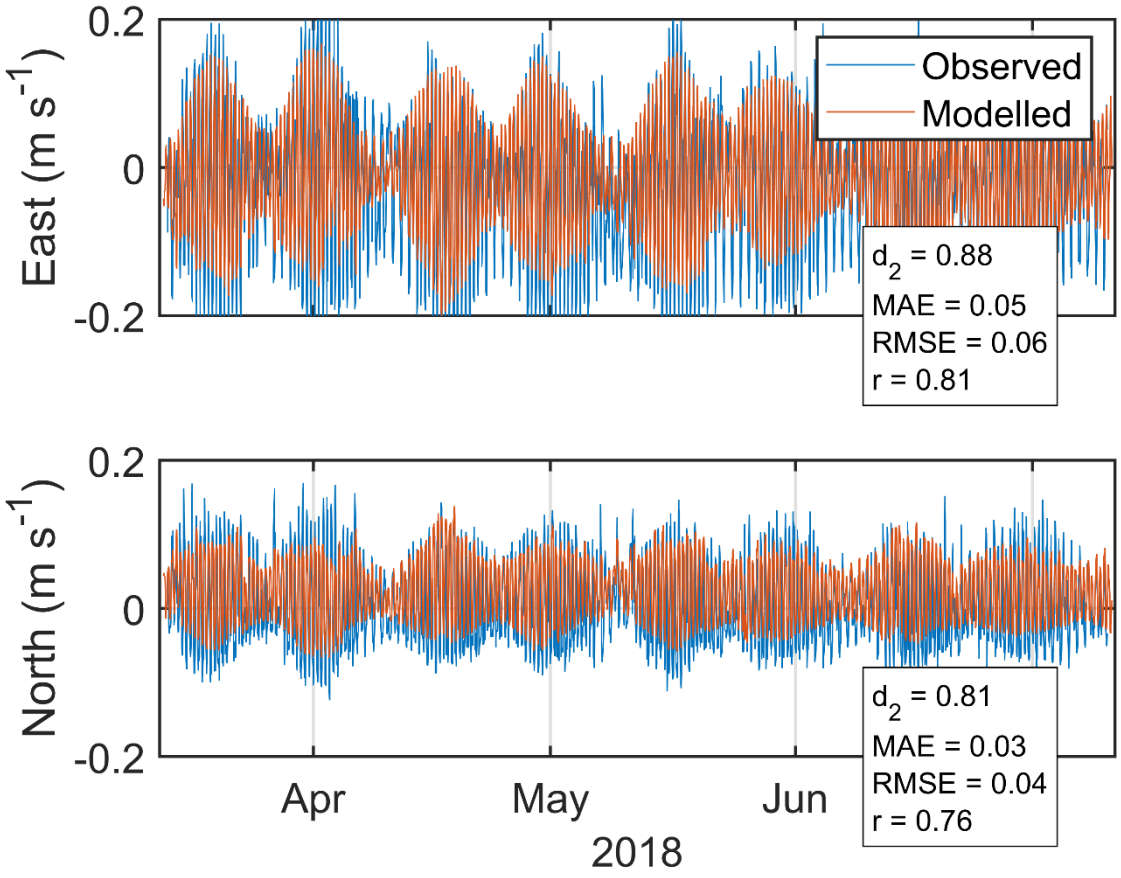

Figure A.3**.** Comparison between observed and modelled East (top) and North (bottom) components of velocity at the ADCP location for 15 days in March – July 2018. Observed data are in blue, model results in red.

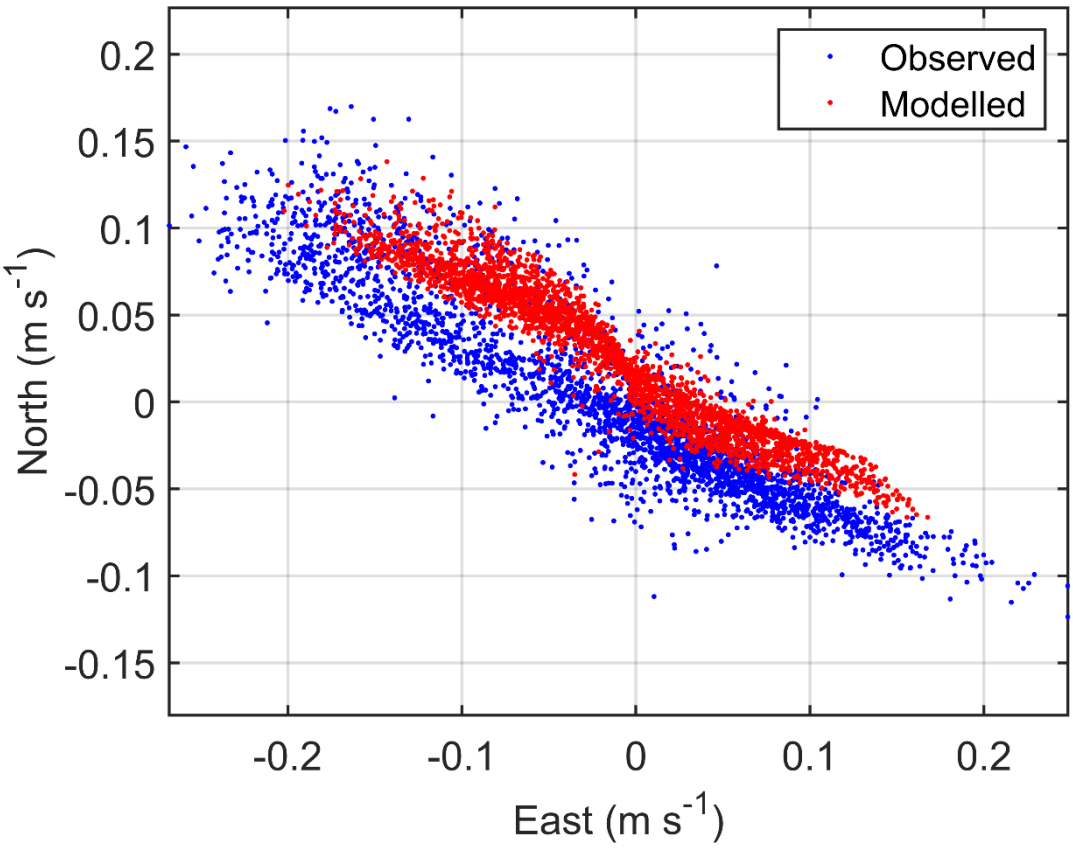

Figure A.4. Scatter plot of observed and modelled velocity at the ADCP location from March - July 2018 (ID210). Observed data are in blue, model results in red.

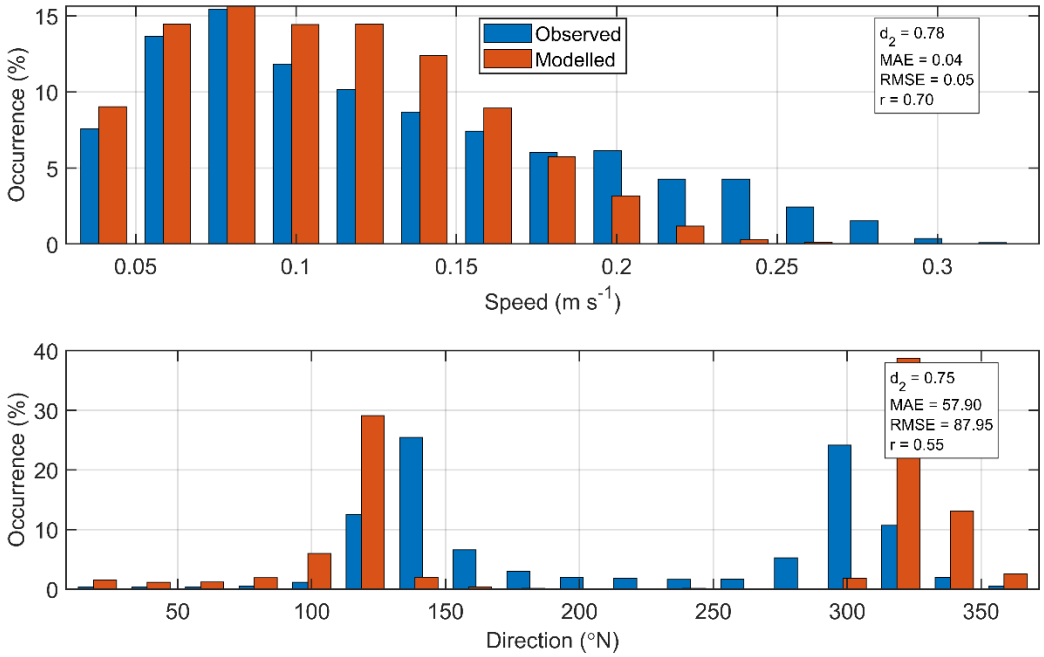

Figure A.5. Histograms of observed and modelled speed (top) and direction (bottom) at the ADCP location from March - July 2018 (ID210). Observed data are in blue, model results in red.

Table A.2. Model performance statistics for sea surface height (SSH), and East and North velocity at the ADCP location from the calibration simulation, March - July 2018 (ID210).

	SSH	East	North
Skill, d_2	0.99	0.88	0.81
Mean Absolute Error (MAE)	0.15 m	0.05 m s^{-1}	0.03 m s^{-1}
Root-Mean-Square Error (RMSE)	0.18 m	0.06 m s^{-1}	0.04 m s^{-1}

A.3.2 Validation, June - August 2020

The model was validated against ADCP data from June - August 2020 (ID342). The validation looks first at sea surface height, as measured by the ADCP pressure sensors, and secondly at the north and east components of velocity. The results of the validation exercise are presented in Figures A.6 – A.9 and Table A.3.

For the validation period, the model performance was not quite as good as for the calibration, but still very adequate. Model skill scores were 0.99, 0.82 and 0.93 for the sea surface height and East and North components of velocity. RMSE values were 0.19 m, 0.09 m s^{-1} and 0.06 m s^{-1} for SSH and the two components of velocity (Table A.3). The scatter plots and histograms demonstrate that the modelled current had broadly the same magnitude and direction characteristics as the observed data (Figures A.8 and A.9).

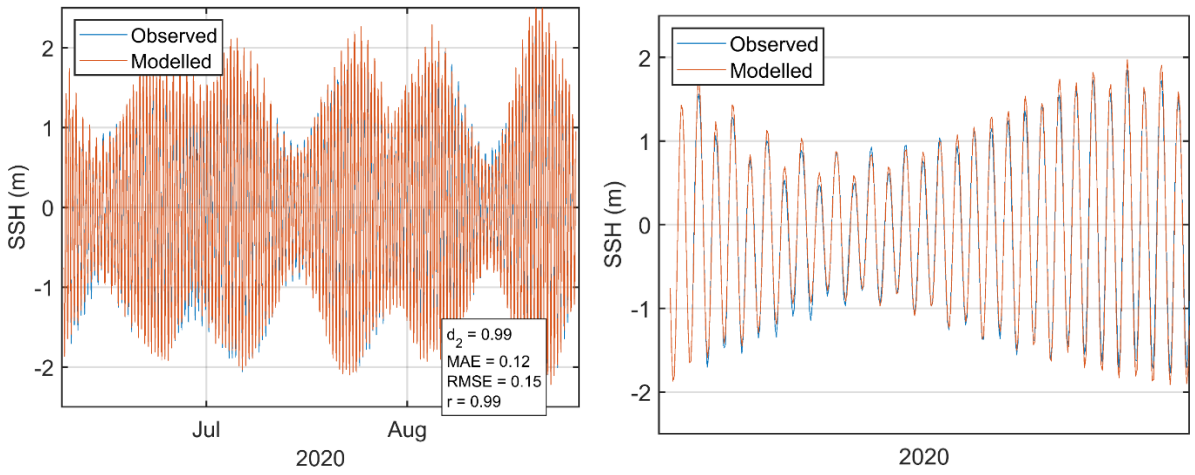

Figure A.6. Comparison between observed and modelled sea surface height at the ADCP location from June - August 2020 using parameter values from Table A.. Both the full record (left) and a subset of 15 days (right) are shown. Observed data are in blue, model results in red.

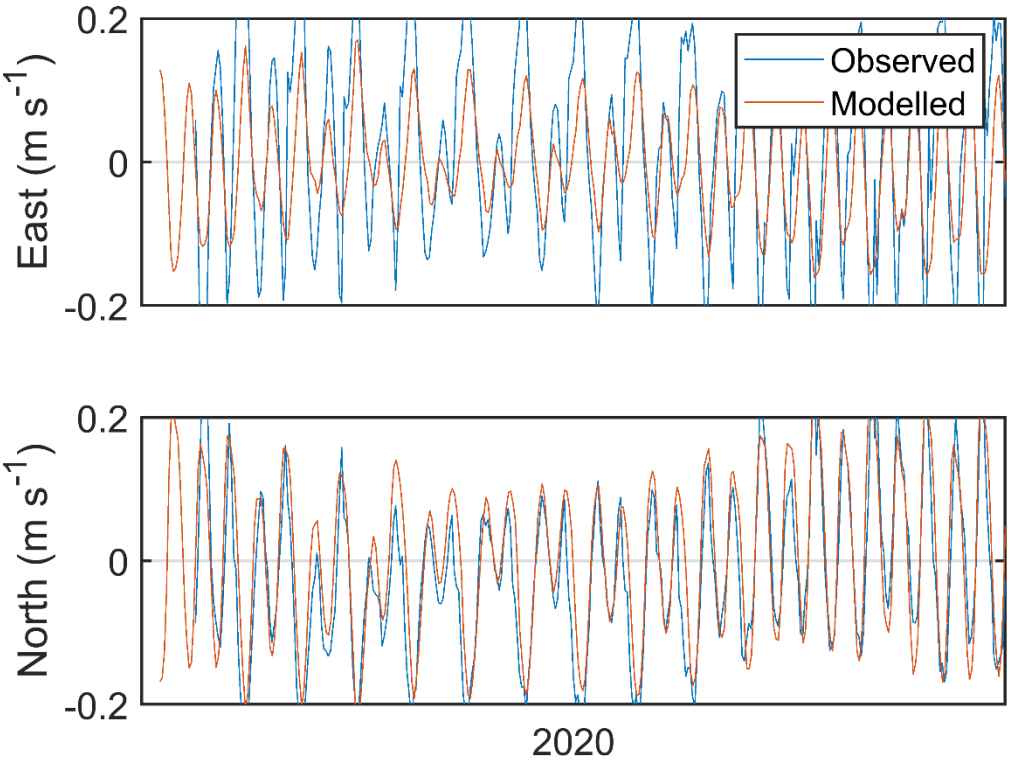

Figure A.7**.** Comparison between observed (ID342) and modelled East (top) and North (bottom) components of velocity at the ADCP location for 15 days in 2020. Observed data are in blue, model results in red.

Table A.3. Model performance statistics for sea surface height (SSH) and East and North velocity at the ADCP location from June - August 2020 (ID342).

	SSH	**East**	**North**
Model skill, d_2	0.99	0.82	0.93
Mean Absolute Error (MAE)	0.12 m	0.07 m s^{-1}	0.05 m s^{-1}
Root-Mean-Square Error (RMSE)	0.19 m	0.09 m s^{-1}	0.06 m s^{-1}

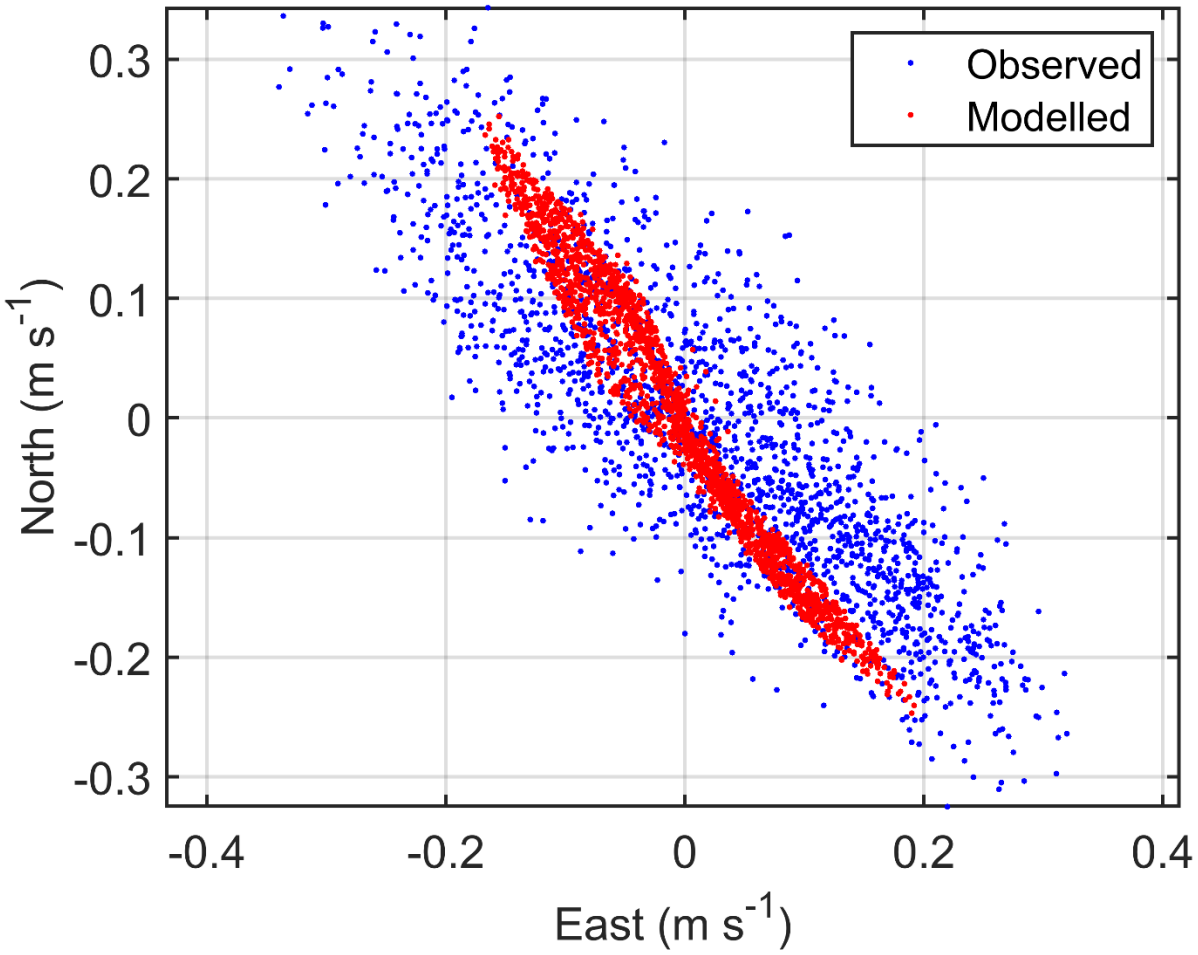

Figure A.8. Scatter plot of observed and modelled velocity at the ADCP location from June – August 2020 (ID342). Observed data are in blue, model results in red.

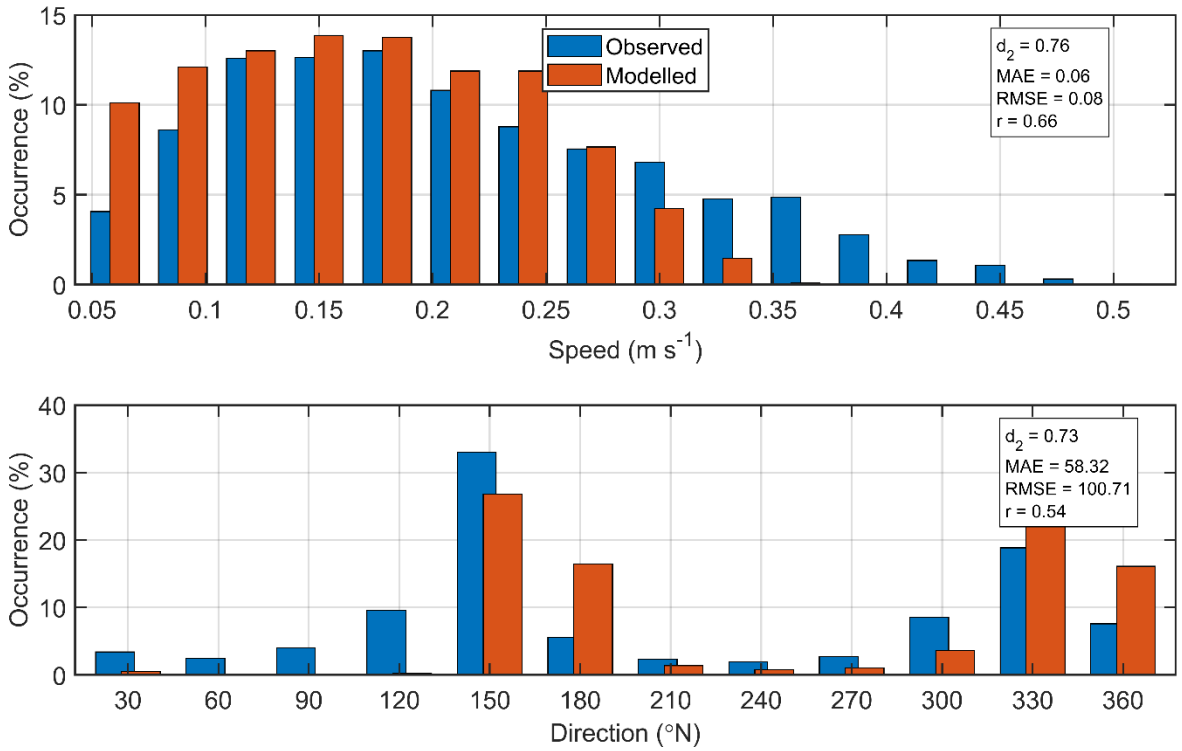

Figure A.9. Histograms of observed and modelled speed (top) and direction (bottom) at the ADCP location from June – August 2020 (ID342). Observed data are in blue, model results in red.

A.4 Modelled Flow Fields

Modelled flood and ebb velocity vectors at spring tides are illustrated in Figure A.14. The Grey Horse Channel site is exposed to the strong currents where the Minch meets the Sound of Harris. The prevailing flow is north-westwards which is typical of the Scottish Coastal Current. The dispersion modelling reflected this regime, with the patches of medicine in every modelled case being transported north-westwards towards the Sound of Harris and the Minch.

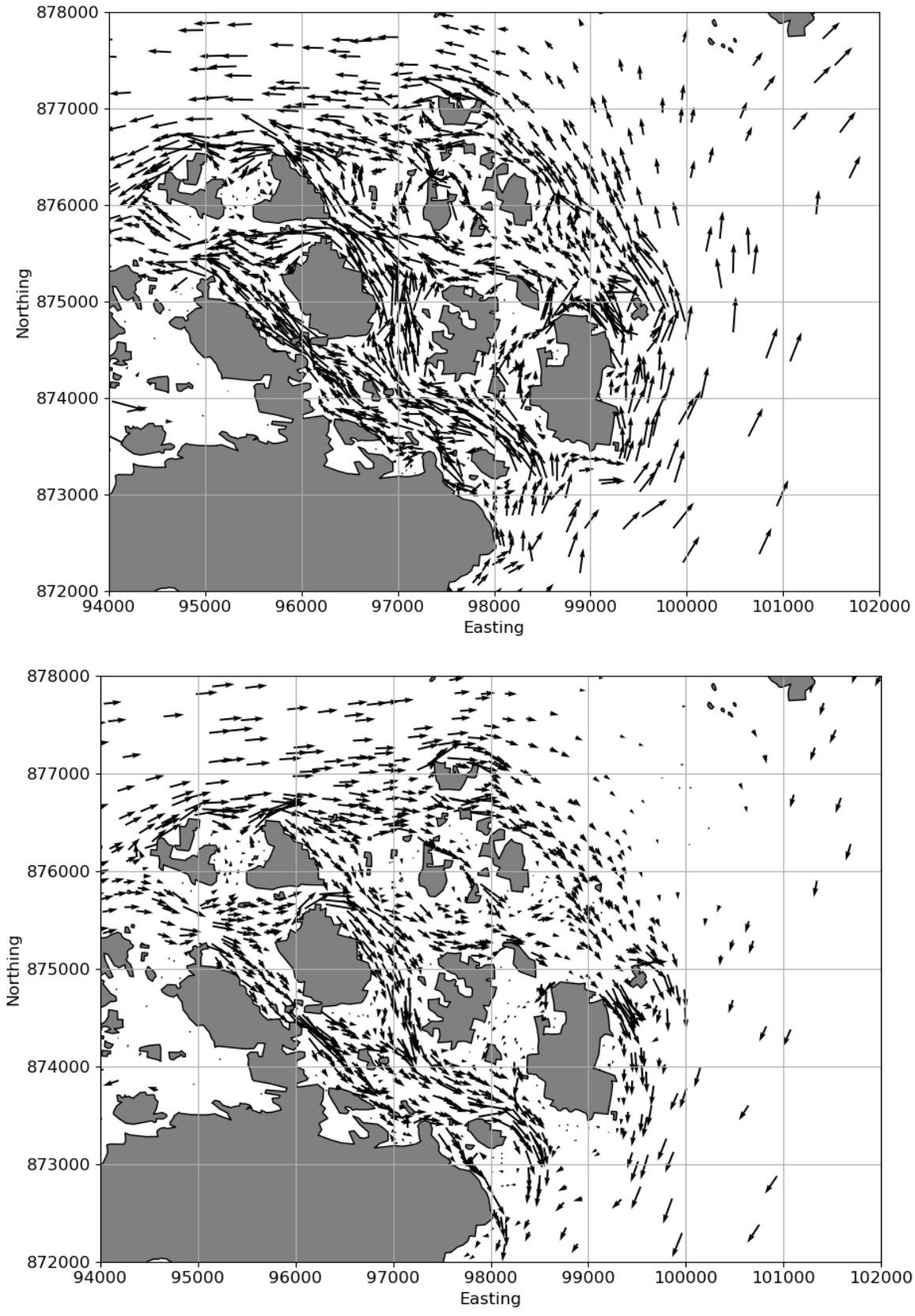

Figure A.10. Modelled flood (top) and ebb (bottom) surface current vectors during spring tides on 14th June 2018. For clarity, only 25% of the model vectors are shown.

A.5 References

Casulli, V. 1987. Eulerian-lagrangian methods for hyperbolic and convection dominated parabolic problems. In: Taylor, C., Owen, D., Hinton, E. (Eds.), Computational Methods for Non-linear Problems, Pineridge Press, Swansea,U.K., pp. 239–268.

Elliott, A.E.; Gillibrand, P.A.; Turrell, W.R 1992. Tidal mixing near the sill of a Scottish sea loch. In *Dynamics and exchanges in estuaries and the coastal zone*, Coastal and Estuarine Studies, 40, D. Prandle (ed.), American Geophysical Union, Washington D.C., pp 35 – 56.

Gillibrand, P.A.; Lane, E.M.; Walters, R.A.; Gorman, R.M. 2011. Forecasting extreme sea surface height and coastal inundation from tides, surge and wave setup. Austr. J. Civil Eng. 9, 99-112.

Gillibrand, P. A.; Turrell, W.R.; Elliott, A.J. 1995. Deep-water renewal in the upper basin of Loch Sunart, a Scottish fjord, J. Phys. Oceanogr., 25, 1488– 1503.

Lane, E.M.; Gillibrand, P.A.; Arnold, J.R.; Walters, R.A. 2011. Tsunami inundation modelling with RiCOM. Austr. J. Civil Eng., 9, 83-98.

Plew, D. R.; Stevens, C. L. 2013. Numerical modelling of the effect of turbines on currents in a tidal channel–Tory Channel, New Zealand. Renew. Energy, 57, 269-282.

Walters, R. A. 2005a. Coastal ocean models: two useful finite element methods. Cont. Shelf Res., 25(7), 775-793.

Walters, R. A. 2005b. A semi-implicit finite element model for non-hydrostatic (dispersive) surface waves. Int. J. Num. Meth. Fluids, 49(7), 721-737.

Walters, R.A. 2016. A coastal ocean model with sub grid approximation. *Ocean Mod*., 102, 45-54.

Walters, R.A.; Gillibrand, P.A.; Bell, R.; Lane, E.M. 2010. A Study of Tides and Currents in Cook Strait, New Zealand. Ocean Dyn., 60, 1559-1580.

Walters, R.A., Lane, E.M., Hanert, E. 2009. Useful time-stepping methods for the Coriolis term in a shallow water model. *Ocean Model*., *28*, 66–74. doi: 10.1016/j. ocemod.20 08.10.0 04.

Walters, R.A. ; Lane, E.M.; Henry, R.F. 2008. Semi-lagrangian methods for a finite element coastal ocean model. *Ocean Model*., 19, 112–124.

Walters, R. A.; Tarbotton, M. R.; Hiles, C. E. 2013. Estimation of tidal power potential. Renew. Energy, 51, 255-262.

Willmott, C. J.; Ackleson, S. G.; Davis, R. E.; Feddema, J. J.; Klink, K. M.; Legates, D. R. O'Donnell, J.; Rowe, C. M. 1985. Statistics for evaluation and comparison of models, J. Geophys. Res., 90, 8995– 9005.

Wu, J. 1982. Wind-stress coefficients over sea surface from breeze to hurricane, J. Geophys. Res., 87(C12), 9704–9706, doi:10.1029/JC087iC12p09704.